Synthesis, Structural and Photophysical Evaluations of Urea based Fluorescent PET Sensors

Thorfinnur Gunnlaugsson

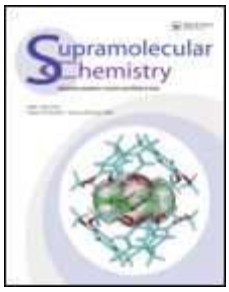

Synthesis, Structural and Photophysical Evaluations of Urea based Fluorescent PET Sensors

Journal:	*Supramolecular Chemistry*
Manuscript ID:	GSCH-2006-0117.R3
Manuscript Type:	Full Paper
Date Submitted by the Author:	17-Feb-2007
Complete List of Authors:	Gunnlaugsson, Thorfinnur; Trinity College Dublin, Chemistry
Keywords:	anion receptors, urea, fluorescence, sensors, chemosensors
Note: The following files were submitted by the author for peer review, but cannot be converted to PDF. You must view these files (e.g. movies) online.	
scheme 1.skc	

Synthesis, Structural and Photophysical Evaluations of Urea based Fluorescent PET Sensors for Anions

Cidália M. G. dos Santos,[a,b] Mark Glynn,[a] Tomas McCabe,[a] J. Sérgio Seixas de Melo,[b] Hugh D. Burrows[b] and Thorfinnur Gunnlaugsson[a*]

a) School of Chemistry, Centre for Synthesis and Chemical Biology, Trinity College Dublin, Dublin 2, Ireland.

b) Departamento de Química, Faculdade de Ciências e Tecnologia, Universidade de Coimbra, Portugal.

Abstract: The design, synthesis and photophysical evaluation of four anthracene based photoinduced electron transfer (PET) sensors (**3a-d**) for anions is described. The [4π+4π] photodimerization product, **4**, was also obtained from **3b**, by slow evaporation from DMSO solution and its X-ray crystal structure determined. The structure of **4**, showed the classical dimerization at the 9,10-positions of anthracene. Sensors **3a-d** are all based on the use of charge neutral aryl urea receptors, where the recognition of anions such as acetate, phosphate and iodide, was found to be due to the formation of strong hydrogen bonding interactions in DMSO. This anion recognition resulted in enhanced quenching of the anthracene excited state *via* electron transfer from the receptor; hence the emission was '*switched on-off*'. The sensing of fluoride was, however, found to be a two-step process, which involved initial hydrogen bonding interactions with the receptor, followed by deprotonation and the formation of bifluoride (HF_2^-). The changes in the emission spectra upon sensing of chloride and bromide were, however, minor. The photophysical properties of these sensors in the presence of various anions were further studied, including investigation of their excited state lifetimes and

* Corresponding author. Phone: +353 1 896 3459. Fax: +353 1 671 2826. E-mail: gunnlaut@tcd.ie

quantum yields, as well as detailed Stern-Volmer kinetic analysis with the aim of determining the dynamic and static quenching constants, k_q and k_s for the above anion recognition. These measurements indicated that while the anion dependant quenching was mostly by a dynamic process, some contribution from static quenching was also observed at lower anion concentrations.

INTRODUCTION

Over the years, much effort has been devoted to the development of selective and sensitive optical chemosensors for real time detection of ions and molecules which are of major interest in clinical analysis and diagnostics, biology and environmental chemistry.[1-3] The sensing of anions has become an important area of research in supramolecular chemistry, with many excellent examples being published in the last few years.[4-6] Particular emphasis has been placed on the use of charge neutral anion receptors such as thioureas, ureas and amidoureas, as well as amides and pyrroles as anion recognition moieties. The incorporation of these into chromophores and fluorophores with the aim of developing colorimetric and fluorescent sensors for anions has become an important area of research.[7-10] Gale *et al.* have been at the forefront of such research and have recently used anion binding motifs such as amidoureas in naked eye detection of biologically important anions, by incorporating these binding moieties as integrated parts of 'push-pull' chromophores, as well as including such anion recognition sites into macrocyclic structures.[11,12] Several other groups, such as Pfeiffer *et al.*[13], He *et al.* [14], Fabbrizzi *et al.*[15] and Jiang *et al.* [16] have also used similar aryl based ureas or thiourea architectures to achieve colorimetric sensing of anions. At the same time, we developed the first examples of charge neutral PET sensors for anions using thiourea receptors.[17] We have also developed sensors using aminourea based receptors for the recognition of anions in aqueous solution, or by incorporating such binding

motifs into preorganized structural scaffolds such as calix[4]arene.[18] We have also demonstrated the fixation of CO_2 as HCO_2^- by using colorimetric anion sensors based on the naphthalimide fluorophore,[19] and have shown that lanthanide (Tb(III) or Eu(III)) luminescent complexes can be employed to detect aromatic or aliphatic mono and bis-carboxylates in competitive media, or by using displacement assays. [20,21]

In our earlier work, which was centred on developing charge neutral fluorescent anion sensors, we focused on the use of anthracene and naphthalimide based sensors, where the changes in the fluorescence intensity of these sensors were monitored upon increased anion concentration.[17,19] We showed that the recognition of these anions, on all occasions, gave rise to reduced emission, which we describe as an '*on-off*' emission changes. We proposed that these changes were due to enhanced photoinduced electron transfer (PET) quenching of the fluorophore excited state from the anion receptor, upon anion recognition. However, a more comprehensive photophysical investigation into this phenomenon has not been carried out in our laboratory, and with this in mind we set out to develop several new fluorescent PET sensors using substituted urea receptors. These sensors, **3a-3d**, are all based on the classical *fluorophore-spacer-receptor* model, where the aryl receptor is separated from the flourophore fluorophore by a short spacer.[22] These are also the first examples of such urea based sensors from our laboratory.

The urea receptors, **3a-3d**, were also selected in such a manner to gain further insight into the effect that the aryl based receptors would have on: *a*) the binding affinity of the receptor and *b*) the efficiency of the electron transfer quenching. Hence, questions such as do the more electron withdrawing receptors give rise to stronger binding and hence more efficient quenching than electron donating ones (as such inductive effects would make the urea protons more acidic and hence, stronger hydrogen bonding donors), had not been fully answered. Herein, we give a full account of our investigation, which involved the titration of

3a-3d with various anions and observing the changes in the various photophysical properties of these compounds upon anion sensing.

RESULTS AND DISCUSSION

Synthesis of compounds 3a-3d

The synthesis of the desired urea based sensors was achieved in high yield in a single step, Scheme 1, from 9-aminomethyl anthracene, **1**, by reacting it with the commercially available isocyanides: 2,4-difluorophenyl-,(**2a**), 4-(trifluoromethyl) phenyl-,(**2b**), 3,5-dimethylphenyl-

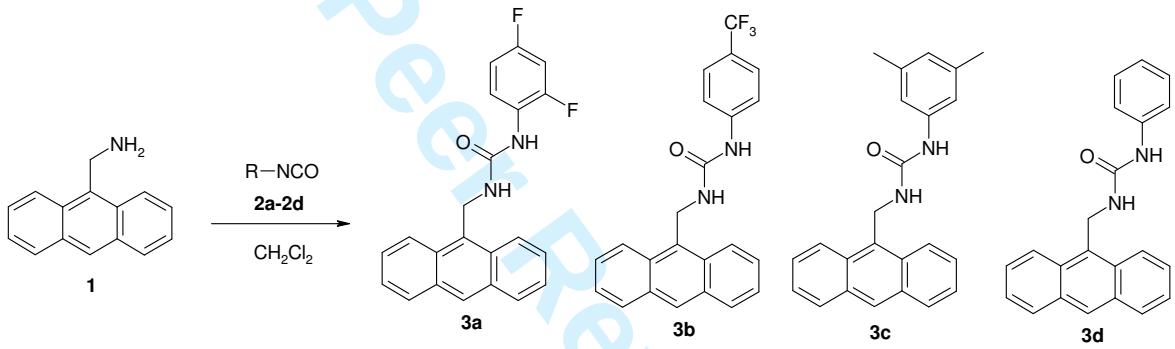

Scheme 1. Synthesis of the urea based anion sensors **3a-3d**. See text for **2a-2d**.

(**2c**) and phenyl- isocyanate, (**2d**), respectively, in dry CH_2Cl_2, at room temperature. In all cases, upon addition of **2a-d** to **1**, creamy pale yellow precipitates were immediately observed. Nevertheless, the reactions were left stirring overnight. The resulting precipitates were then collected by suction filtration, washed several times with cold CH_2Cl_2 and dried under high vacuum. Compounds **3a-d** were all obtained in yields of 80-97% after recrystallisation from $CHCl_3$. All the compounds were characterised using conventional methods (see experimental section). The sensors were partially soluble in $CDCl_3$, and fully soluble in DMSO-d_6. In the latter solvent, two characteristic resonances were observed at 8.47 ppm and 8.45 ppm, for the urea protons of the electron deficient **3a**, while for the electron rich sensor **3d** these protons apperad at 8. 14 ppm and 6.61 ppm.

The X-ray crystal structure analysis of [2+2] photochemical adduct of 3b

Several attempts were made to obtain crystals of the above sensors for X-ray crystal structure analysis. However, the use of slow evaporation or diffusion techniques failed on all occasions. In contrast, colourless crystals were obtained from an NMR sample of **3b**, in DMSO-d_6, and were found to be suitable for X-ray crystal structure analysis.[23,24] Although, to our

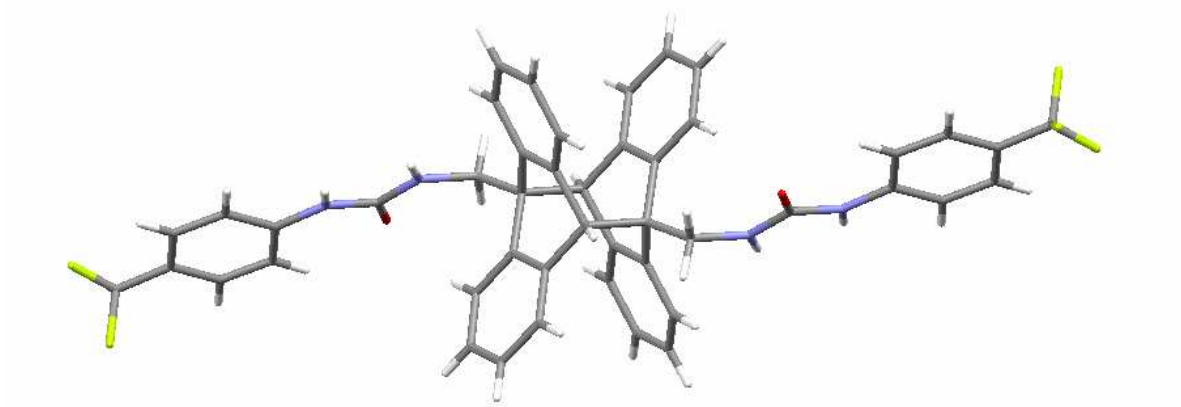

Figure 1. The X-ray crystal structure of the [4π+4π] cyclcoaddition product **4**, formed from **3b**. A DMSO molecule has been removed for clarity (see text).

surprise, the structure was not that of the desired sensor **3b**, but the product of the resulting [4π+4π] photocycloaddition dimerization reaction between two molecules of **3b**, *i.e.* **4**. The new bonds were formed between the central rings on each anthracene unit as is evident from Figure 1. It also shows that the structure adopts C_2 symmetry with the two urea receptors being *anti* to each other, with a single DMSO molecule being found in the unit cell. This structure can only be obtained photochemically, which is however, thermally reversible, and only from the desired compound **3b**. Hence, **4** can be viewed as being the proof of the formation of **3b**. This photochemical reaction is a common phenomenon for anthracene, which can be dimerized easily upon UV radiation.[25,26] However, the sample that these crystals were grown from was only exposed to halogen based room-light and/or sunlight. We therefore propose that the urea receptor activates the 9 position of the anthracene sensor **3b** in such a way that it dimerizes in this manner. The structure of **4**, is one of two possible structural isomers; the other being where the two receptors would be on the same side ('*syn*'

to each other) of the photodimerised product of **3b**. This is also known as the *head-to-tail* product.[25,26] Compound **4**, is however, the so called tail-to-tail product, and is described as being the more stable of the two isomers. It is usually the product isolated upon photodimerization of such 9-substituted anthracene molecules. This is also believed to be the more thermally reversible product. As is typical for such dimerization products, the four aryl rings adopt a double wing like appearance, with a C…C bond length of 1.626(4) Å between the two former anthracene 9 and 10 positions. Moreover, the bond angle between the C9-C30-C17 atoms was found to be on average 113.1°, which is also typical for such products. The structure also shows that the urea moieties are almost coplanar with the 4-(trifluoromethyl) phenyl groups, with average N…H bond length of 0.860Å.

The packing diagram of **4** viewed down the crystallographic c axes can be seen in Figure 2. This shows that each of the urea moieties is hydrogen bonded to the oxygen of an aforementioned DMSO molecule, with a O…H bond length of 2.95 Å. However, even

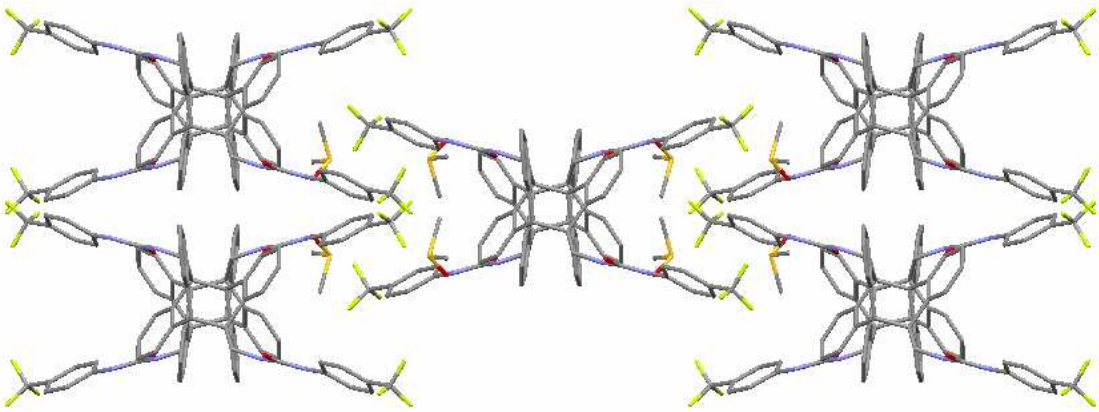

Figure 2. The packing diagram for **4** by viewing down the c-axis. Hydrogen atoms and short-contacts have been removed for clarity.

though the 4-(trifluoromethyl) phenyl groups show evidence of stacking, the distance between the two aryl groups is 8.7Å, which is too long to account for any π–π stacking interactions. There is however, a further F…H interaction between the aryl CF_3 groups and the protons of

the DMSO molecules with average F…H distance of 2.66 Å. The anion recognition ability of this structure was not evaluated.

Photophysical evaluation of 3a-3d

The photophysical properties of the four sensors were evaluated in DMSO. The ground state properties of **3a-3d** were first investigated. The absorption spectra of all the sensors were almost identical, when recorded in DMSO, with bands appearing at 340, 369 and 324 nm, respectively, and a shoulder at 333 nm which was assigned to the aryl groups of the receptor moieties. These are significantly shifted towards the red in comparison with anthracene, which has three characteristic bands appearing at 342, 360 and 380 nm, respectively.[27] For these four sensors, extinction coefficients of 9920, 10830, 7279 and 9560 [$Mol^{-1}cm^{-1}$] were determined in DMSO for **3a-3d**, respectively.

Using for excitation, the 369 nm transition of the anthracene based sensors, and the 360 nm band of the reference anthracene chromophore, the fluorescence emission spectra were recorded in DMSO. Here, the characteristic fluorescence emission of the anthracene fluorophore was observed for all the compounds, with that of the sensors being red-shifted by

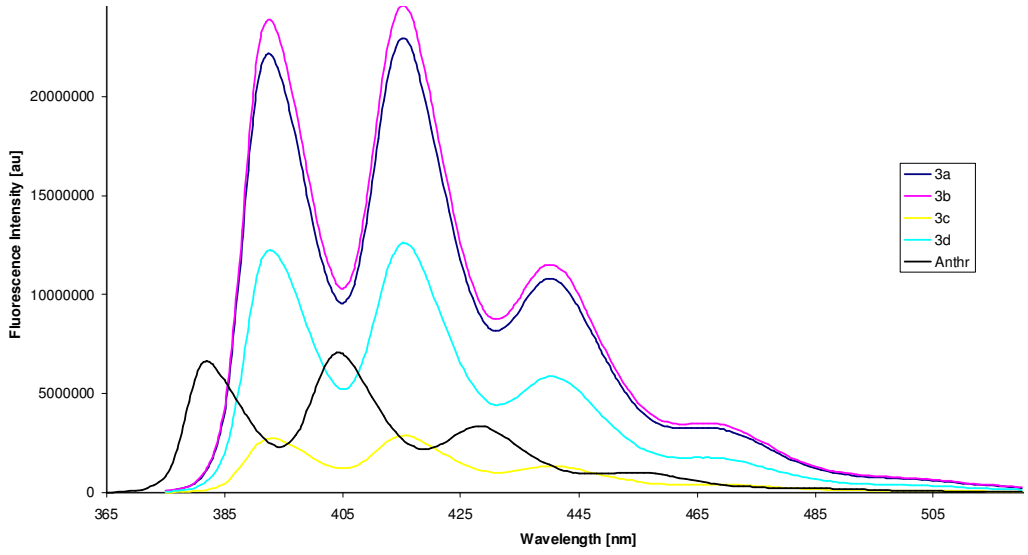

Figure 3. Comparison between the fluorescence emission spectra of chemosensors **3a-d** and the spectrum of anthracene, **Anthr**, in DMSO.

ca. 10 nm in comparison with that of anthracene itself, Figure 3, emitting at 393, 415 and 440 nm, with a shoulder at 466 nm. As can be seen from Figure 3, the intensity of all the sensors, with the exception of **3c**, was greater than that of the reference anthracene compound. For **3a-3d** the quantum yields of fluorescence (Φ_F) were determined as 0.53, 0.57, 0.06 and 0.33, respectively under these experimental conditions, where the order is **3a>3b>3d>3c**, which shows that the more electron withdrawing substituents give rise to the higher quantum yields. This follows a known trend, where 9,10-dimethyl anthracene has a higher quantum yield than 9-methyl-anthrancene, which subsequently has higher quantum yield than anthracene itself. However, and perhaps somewhat surprising, then it is worth noting that in the case of **3c**, the di-substitution at the aryl ring gives rise to a very low quantum yield in comparison the rest of the sensors. A similar trend was seen for the fluorescence lifetimes (τ_F) in DMSO. The decays upon excitation of the 356 nm transition and observation at 450 nm were all single exponential, and had lifetimes 7.83, 8.99, 1.32 and 4.96 ns, respectively for the sensors **3a-3d.** From these changes, the rate constants for fluorescence k_F, can be determined, as being 6.76×10^7, 6.34×10^7, 4.55×10^7 and $6.67\times10^7 s^{-1}$ for **3a-3d**, respectively. From these results it is clear, that even though there is no significant difference in either the λ_{Absmax} or λ_{Fmax} for these sensors, the anion urea receptors have a significant effect on both Φ_F and τ_F. This is most pronounced for the electron rich reporter system **3c**, where Φ_F and τ_F are significantly lower than that observed for the remaining sensors. This is most likely to be due to a more efficient photoinduced electron transfer quenching of the anthracene excited state by **3c**, in its 'free' form (in the absence of any anions), while the electron withdrawing substituents of **3a** and **3b** make the aromatic urea electron deficient and hence less able to participate in PET quenching. This is supported by the fact that the results obtained for sensor **3d**, follow this trend, where both the Φ_F and τ_F are smaller than that of **3a** and **3b**, but larger than that of **3c**. It is also

worth noting that **3a** and **3b**, which have electron withdrawing substituents on their receptors, seem to have very similar photophysical properties.

Anion binding evaluations of compounds 3a-3d

Having established the fundamental photophysical properties of compounds **3a-3d**, the four compounds synthesised above were evaluated for their ability to detect anions in DMSO, by observing the changes in both the absorption and fluorescence emission spectra upon titrating these sensors with stock solutions of AcO^-, $H_2PO_4^-$, F^-, Cl^-, Br^- and I^- (as their tetrabutyl ammonium salts). Upon titration of these sensors with anions such as AcO^-, $H_2PO_4^-$, F^-, only minor changes were seen in the absorption spectra for the anthracene component at longer wavelengths, while more significant changes were seen at shorter wavelengths. While

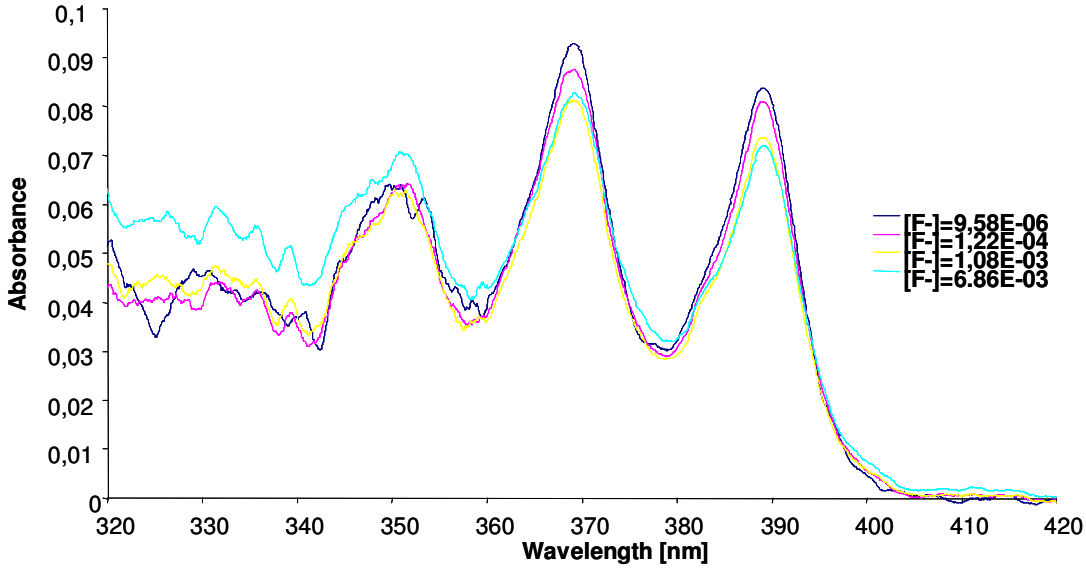

Figure 4. The changes in the absorption spectra of **3a** upon titration with F^- upon excitation of 369 nm, in DMSO.

these latter changes were assigned to the interaction of the anion at the urea receptor, the lack of changes in the anthracene transitions is not all together surprising as the methylene spacer should prevent any significant ground state interactions between the two parts. This is clear from Figure 4 which shows the titration of **3a** with F^-, where the major changes in the

absorption spectra occur at short wavelengths, indicating direct interaction between the receptor and the anion through hydrogen bonding.

Similar results were observed for $H_2PO_4^-$. When these measurements were made using AcO^- the changes in the shorter wavelengths were more pronounced. In comparison to these changes, the absorption spectra of **3a-3d** were not affected by the addition of either Cl^- or Br^-. However, upon titration of these sensors with I^- no significant changes were observed in the absorption spectra at low and medium concentrations (0→ 3 mM), while at high concentrations (~ 0.02M) the fine structure of the absorption spectra was displaced by an intense, broad structure, signifying strong ground state interactions between these sensors and I^- under these conditions. In general, the changes in the absorption spectra of the fluorophore, with the exception of I^- can be considered to be minor and only the changes at short wavelengths, assigned to that of the receptor are affected. This indicates that anions such as AcO^-, $H_2PO_4^-$, F^- only interact with the receptor part of the sensors and that the methylene spacer prevents any ground state interactions between the fluorophore and the receptor.

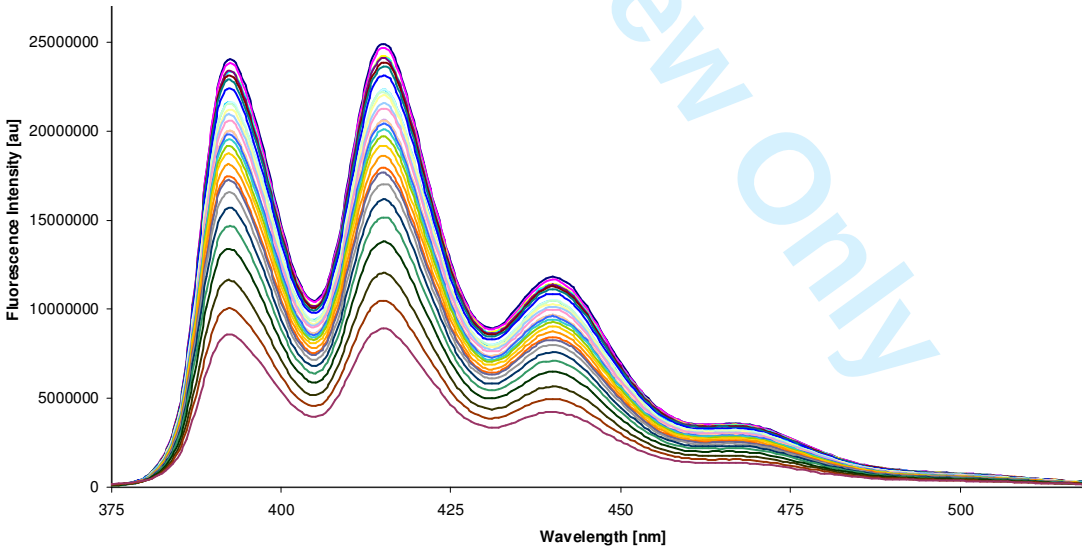

Figure 5. Fluorescence emission of **3a** titrated with TBAAcO, from top to bottom $[AcO^-]$= 0 to 6.27×10^{-2} M. From values of the fluorescence intensity at 415nm the value for the quenching extent was measured to be *ca.* 64%.

Hence, it can be concluded that these urea based sensors behave as 'ideal' PET sensors for anions.

In contrast to the changes in the absorption spectra, the anthracene based emission was significantly modulated upon titration with the above anions in DMSO. The changes observed for the titration of **3a** with AcO^-, is shown in Figures 5. It clearly demonstrates that the emission is quenched upon addition of AcO^-, signifying the recognition of the anion at the receptor side. It is also noticeable, that only the intensity of fluorescence is modulated and no significant changes are observed in the positions of the three characteristic anthracene emission bands. It can thus be concluded that these sensors behave as PET sensors, where the emission of the fluorophore is quenched by PET from the receptor to the excited sate of the fluorophore.

Unlike that observed for classical PET cation sensors, where the emission is enhanced due to the suppression of PET, caused by the increased oxidation potential of the receptor upon cation recognition, the emission here is reduced. This can be viewed as a result of the formation of a more electron rich anion-receptor complex, which gives rise to the enhancement of the reduction potential. As Figure 5 demonstrates, the changes in the emission spectra were homogenous across all the wavelengths, *i.e.* no particular transition was more reduced than the other. Consequently, by observing the changes in the 414 nm transition as a function of $\log[AcO^-]$, a sigmoidal plot was obtained, from which a binding constant $\log \beta$ was determined to be *ca.* 2. By plotting $\text{Log } [(I_{max}-I_F)/(I_F-I_{min})]$ as a function of $\log[AcO^-]$, a linear plot ($R^2 = 0.92$) was observed from which a $\log \beta = 2.14$ (±0.1) was determined.[28] This indicates a week binding between the sensor and the anion. When the same titrations were carried out using **3b-3d**, similar luminescent changes were observed, where the emission was quenched upon increasing anion concentration, without any measurable changes in λ_{max}. From these changes, binding constants of 2.44(±01), 2.07(±01) and 2.09(±01) were

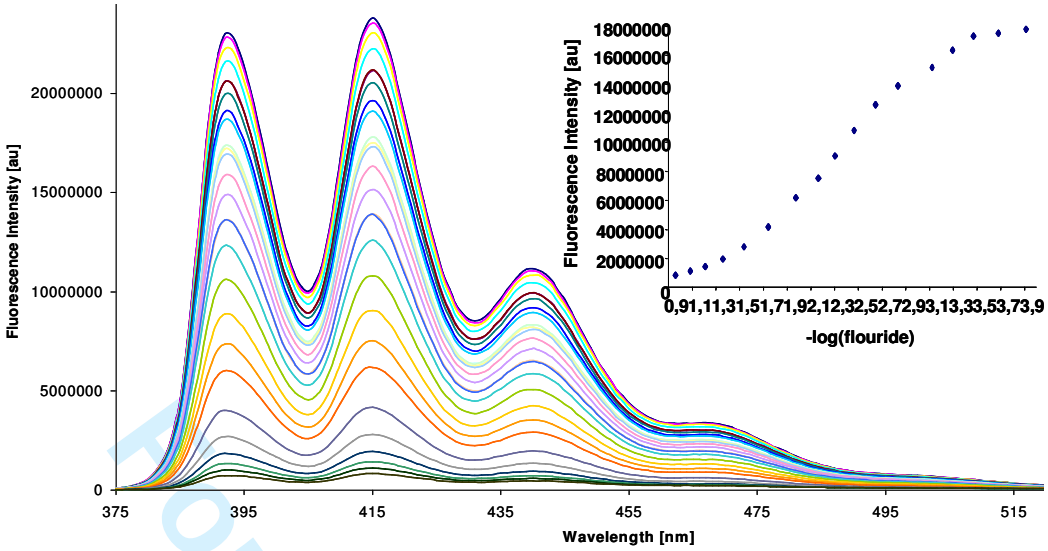

Figure 6. Fluorescence titration spectra showing the changes in fluorescence emission of **3a** in DMSO upon addition of fluoride, from top to bottom, $[F^-]= 0 \rightarrow 1.1\times10^{-1}$ M. Insert: The changes in the 415 nm transition as a function of $[F^-]$.

determined, for **3b-3d**, respectively. However, for all of these the quenching was more efficient than seen for **3a**, being 81%, 70% and 83% for these three sensors, respectively. The effect of the substituent on the aryl urea receptor can also be seen from these changes. However, these are not as dramatic as one would anticipate. While the binding affinity follows the trend of **3b>3a>3c ~3d**, displaying a marginally stronger binding for the two electron deficient receptors, there is no significant difference in these values. Hence, while the electron withdrawing groups would be expected to make the urea protons more acidic and as such, better hydrogen receptor, the difference in the binding constants does not reflect this. When these titrations were repeated using $H_2PO_4^-$, similar effects were observed. However, the degree of quenching was less, being 50%, 65%, 60% and 57% for the four sensors, respectively. From these changes binding constants (log β) of 1.91(±0.1), 2.11(±0.1), 1.90(±0.1), and 1.96(±0.1), were determined which follow the same trend as seen previously for acetate. When either Cl^- or Br^- were used, the emission was only partially quenched, and only at high concentrations. However, these changes were too small for accurate binding constant determination. We assign this quenching to the formation of a hydrogen bonding

complex between the anion and the receptor rather than being due to heavy atom affect quenching.

The titration of **3a-3d**, using F^- gave similar luminescent changes, *e.g.* no spectral shifts were observed and only the fluorescence emission was quenched, demonstrating effective PET quenching from the receptor upon anion recognition. However, unlike that seen above, the emission was almost fully quenched. This can be seen in Figure 6, for **3a**, which shows that the anthracene emission is reduced by almost 90% at the end of the titration. Similarly, the emission was quenched for **3b-3d**, where it was reduced by *ca*. 97%, 91% and 97%, respectively. From these changes, the binding constants log β of 2.73(±0.1), 3.26(±0.1), 2.59(±0.1) and 2.99(±0.1), were determined.

While the same trend is observed here as above, the binding constants as well as the efficiency of the quenching are significantly higher than seen for either AcO^- or $H_2PO_4^-$. We have previously postulated that this is due to two main phenomena. Firstly, the small ion has higher charge density than either AcO^- or $H_2PO_4^-$ and can form stronger hydrogen bonding complexes with the receptor. Secondly, F^- is a good base in DMSO.[27] Consequently, F^- can possibly deprotonate the urea receptor. This, has been shown to occur through a two step mechanism, which gives rise to the formation of bifluoride, HF_2^-, the formation of which can be monitored by NMR.[29] Moreover, the formation of such species in anion complexes has recently been demonstrated using X-ray crystallography.[30] This deprotonation results in the formation of a highly electron rich receptor, which consequently is also a more efficient PET quencher. It is also possible that the HF_2^- products form a very strong ground state complex with the receptor. With the aim of firmly establishing the nature of the quenching, we decided to determine the rate of the quenching process for all of the sensors using the aforementioned anions.

Kinetics of fluorescence quenching

In order to obtain the quenching rate constants, k_q, from fluorescence intensity measurements at different anion concentrations, [Q], the Stern-Volmer kinetics was followed, **Equation (1)**, where I_0 and I are the fluorescence emission in the absence of quencher (anion) and for a given concentration of anion [Q], respectively, K_{sv} and k_q are the Stern-Volmer and quenching rate constants respectively ($K_{sv} = k_q\ \tau_0$) and τ_0 is the lifetime in the absence of quencher.[27] Here the plot of I_0/I versus the anion concentration should be linear with a slope equal to $k_q\tau_0$. In Figure 7, the results for the titration of **3a** with F^- are shown. A

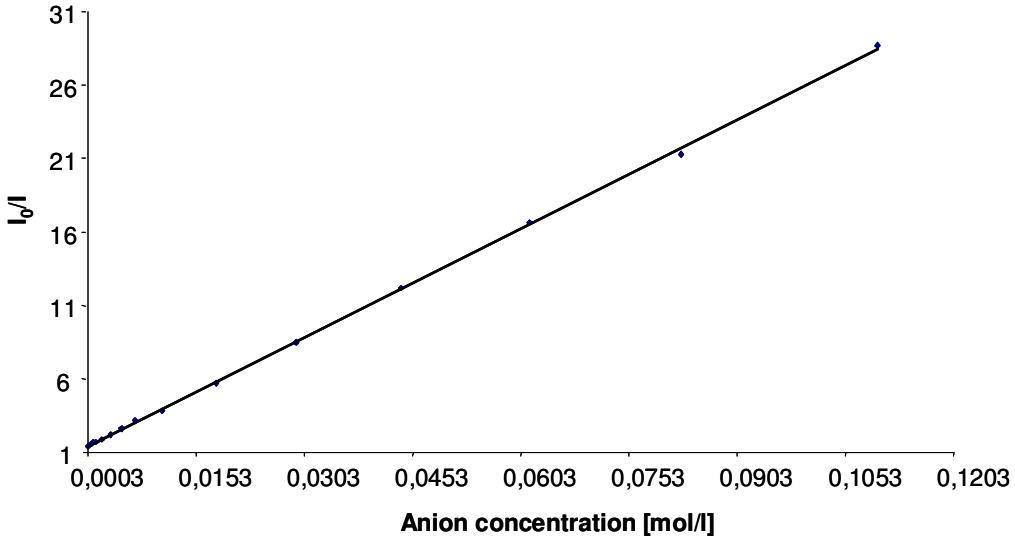

Figure 7. Stern-Volmer plot for the fluorescence quenching of **3a** by F^-. The solid line translates the theoretical curve from the Stern-Volmer **Equation (1)**.

quantitative analysis of the data, based on **Equation (1)**, yielded a Stern-Volmer constant, K_{sv} = 246.68 M^{-1}. The fluorescence lifetime of **3a**, τ_0, was previously determined as being 7.83 ns. Using this lifetime, the quenching constant was found to be $k_q = 3.15 \times 10^{10}\ M^{-1}\ s^{-1}$. The good correlation coefficient obtained leads us to believe that, apparently, a linear behaviour was followed.

$$\frac{I_0}{I} = \left(1 + K_{SV}[Q]\right) = \left(1 + k_q\tau_0[Q]\right) \qquad \textbf{(1)}$$

However, a more detailed study of the Stern-Volmer plot shows that this linearity was not in fact apparent at a low concentration of F^-. As can be seen in Figure 8, the linear behaviour of the Stern-Volmer equation was not observed on the titration of **3a**. This observation can be stated, not only to this experiment, but to all our other experiments. The deviation of the Stern-Volmer equation from linearity can be explained if we consider an alternative quenching process to the dynamic quenching. Hence, the quenching of the fluorescence emission can also arise from static quenching, which can be considered to be due to the interaction between the receptor and the sensor in the ground state, prior to excitation, or dynamic quenching, with formation of a complex between the excited sensor, and the anion receptor. Because of this, both the static and dynamic quenching effects were taken into account in the modified Stern-Volmer equation, **Equation (2)**, where k_s is an equilibrium constant for the static quenching. [31]

$$\frac{I_0}{I} = \left(1 + K_{SV}[Q]\right)\left(1 + k_S[Q]\right) = 1 + \left(k_S + k_q\tau_0\right)[Q] + k_S k_q \tau_0 [Q]^2 \qquad (2)$$

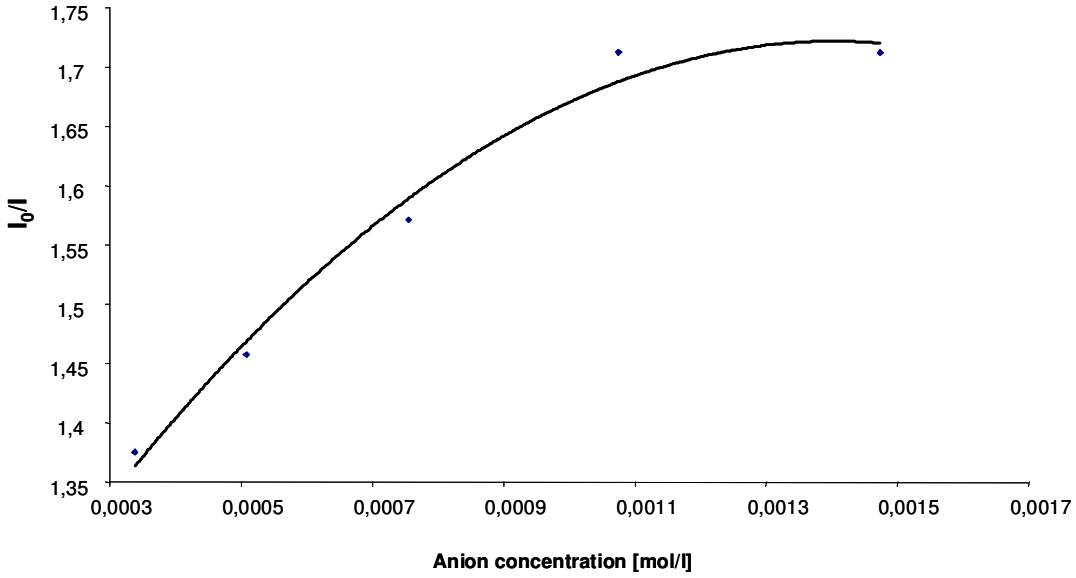

Figure 8. Fraction of the Stern-Volmer plot for the fluorescence quenching of **3a** upon anion, F^-, titration

Using this equation, the kinetics of the fluorescence quenching were re-fitted, by using τ_0, 7.83×10^{-9} s and both the dynamic and static quenching constants, k_q and k_s, determined. For these changes, the values for k_q and k_s were found to be: $k_q = 3.09 \times 10^{10}$ M^{-1} s^{-1}, $k_s = 0.22$ M^{-1}. Even though these are not very significant, from what we observed above, the results do suggests the presence of the static quenching which implies that the sensor is interacting with the anion both in the ground and excited state with a dynamic quenching rate constant close to the diffusion controlled values.

In order to differentiate the dynamic quenching constant obtained using **Equation (1)** from the one obtained using **Equation (2)**, the terms k_{qsv} and k_q were used respectively. The values of K_{sv} and consequently k_{qsv} (dynamic quenching constant based on $K_{sv} = k_{qsv}\ \tau_0$), k_q and k_s found for the fluorescence titrations of **3a-d** with F^-, I^-, AcO^- and $H_2PO_4^-$, following the same method, are summarised in **Table 1**. Since the lifetimes are not dependent on the static quenching, the fluorescence lifetimes shown in **Table 1** for **3a-3d** as a function of the anion concentrations have been measured and analysed according to the **Equation (3)**, where τ_0 and τ are respectively the lifetimes in the absence and presence of quencher (same as reported above).

$$\frac{\tau_0}{\tau} = 1 + k_q \tau_0 [Q] \qquad (3)$$

Table 1. Results form the kinetic investigation for the anion induced quenching of **3a-3d.**

Sensor	τ_0 [ns]	Anion	K_{sv} [M^{-1}]	k_{qsv} [$M^{-1}s^{-1}$]	k_q [$M^{-1}s^{-1}$]	k_s [M^{-1}]
3a	7.83	F^-	246.68	3.15×10^{10}	3.09×10^{10}	0.22
		I^-	79.17	1.01×10^{10}	4.63×10^{9}	9.77
		AcO^-	25.11	3.21×10^{9}	3.67×10^{9}	1.42.*
		$H_2PO_4^-$	8.86	1.79×10^{9}	4.47×10^{9}	6.91 *

3b	8.99	F^-	773.66	8.61×10^{10}	1.27×10^{11}	8.43 *
		I^-	58.68	6.53×10^{9}	4.08×10^{9}	6.03
		AcO^-	93.72	1.04×10^{10}	1.63×10^{10}	7.55 *
		$H_2PO_4^-$	35.02	3.9×10^{9}	7.73×10^{9}	8.84 *
3c	1.32	F^-	158.31	1.2×10^{11}	2.68×10^{11}	9.14 *
		I^-	14.78	1.12×10^{10}	1.34×10^{10}	1.11 *
		AcO^-	59.41	4.5×10^{10}	8.89×10^{10}	13.53 *
		$H_2PO_4^-$	24.67	1.87×10^{10}	2.6×10^{10}	3.82 *
3d	4.96	F^-	452.87	9.13×10^{10}	1.19×10^{11}	3.87 *
		I^-	25.99	5.24×10^{9}	6.91×10^{9}	2.21 *
		AcO^-	99.09	1.2×10^{10}	2.04×10^{10}	0.45 *
		$H_2PO_4^-$	24.94	5.03×10^{9}	9.8×10^{9}	7.89 *

K_{sv} and consequently k_{qsv}, k_q and k_s values found for the fluorescence titrations of **3a-d** with F^-, I^-, AcO^- and $H_2PO_4^-$. *All these values were taken as module as the values were found, following the method described above, to be negative.

From the results in Table 1, it is clear that the fluoride anion gives rise to large $\mathbf{K_{SV}}$, even though its value changes dramatically within this set of sensors. Moreover, these values are about an order of magnitude greater than diffusion control. This is, probably due to, and as discussed earlier, the fact that the there is some degree of ion pairing of bifluoride with the recptor. With the exception of I^-, which has significant ground state interactions with the fluorophores, the same order was observed (as expected) as above with $AcO^- > H_2PO_4^-$. These results also show that the quenching is on all occasion fast and dominated by dynamic quenching, except at low concentrations.

CONCLUSION

We have synthesised several new simple fluorescent PET anion sensors, **3a-d**. These were characterised using conventional techniques as well as the crystal structure of the dimerized [4π+4π] photocycloaddition product of **3b**. These sensors display 'ideal' PET behaviour upon

anion recognition, since only the fluorescence emission is "*switched off*" in the presence of $H_2PO_4^-$, AcO^-, and F^- in DMSO. Hence, the changes in the ground state were only minor and occurred at short wavelengths, which we associate with the interactions of the anions with the receptor, which modulates the receptors redox potential. These sensors also showed good selectivity with AcO^- being recognised over $H_2PO_4^-$. Nevertheless, **3a-d** all showed higher affinity and more efficient quenching for F^-. This is not all together surprising since fluoride high charge density and small size enables it to form strong hydrogen bonds with the urea receptor. Moreover, the anion can deprotonate the receptors, forming HF_2^- which makes the receptor a significantly stronger electron donor and hence an efficient quencher. We also observed significant changes for the titration of I^-. However, these were deemed to be mainly due to ground state interactions between the sensor and the anion. The absorption spectra of all the sensors were shifted to longer wavelengths in comparison to anthracene. Moreover, all the sensors, with the exception of **3c**, gave rise to larger quantum yields of fluorescence, and were also red shifted. A more detailed evaluation of the quenching process using the Stern-Volmer equation showed that generally the expected linearity was up held confirming dynamic quenching. However, closer examination for all the anions showed that at lower anion concentration, static quenching was also observed.

ACKNOWLEDGMENTS

We thank Trinity College Dublin, Universidade de Coimbra, and IRCSET for financial support. We also like to thank Dr. John E. O'Brien for his help.

EXPERIMENTAL

General:

Reagents (obtained from Aldrich) and solvents were purified using standard techniques. Melting points were determined using a GallenKamp melting point apparatus. Infrared spectra were recorded on a Mattson Genesis II FTIR spectrophotometer equipped with a Gateway 2000 4DX2-66 workstation. ^{1}H NMR spectra were recorded at 400 MHz using a Bruker Spectrospin DPX-400 instrument. ^{13}C NMR spectra were recorded at 100 MHz using a Bruker Spectrospin DPX-400 instrument.

Spectroscopic studies:

All measurements were made at room temperature. Fluorescence spectra were measured using a Jovin Ivon-Spex-Fluorolog 3-2.2; the excitation wavelength was 369 nm, the excitation and emission slit widths were 0.5 mm. Emission spectra were corrected for the instrumental response of the system. The absorption spectra were recorded on a Shimadzu UV-2100 spectrophotometer. All absorption and fluorescence spectra were obtained from a solution of the sensor in DMSO in both the absence and the presence of anion guests. The effect of anions on the sensors was investigated by addition of different volumes of an anion (Br^-, Cl^-, I^-, F^-, AcO^-, $H_2PO_4^-$) solution in DMSO, with different concentrations (10^{-5}M to 1M), to a 2ml solution of **3a-d** in DMSO. In each case, for the fluorescence spectra, additions were accompanied with magnetic stirring. All titrations were repeated two times to ensure reproducibility. All the anions were used in the form of their tetrabutylammonium salts [(TBA), $(C_4H_9)_4N^+$]. These salts were purchased from Aldrich and used without further purification. DMSO was purchased from Riedel-Häen and stored over molecular sieves prior to use.

Fluorescence decay measurements were carried out using a home-built TCSPC apparatus with an N_2 filled IBH 5000 coaxial flash lamp as excitation source, Jobin-Ivon monochromators, Philips XP2020Q photomultiplier, and Canberra instruments TAC and MCA. [32, 33] Alternate measurements (1000 c.p.c.) of the pulse profile at 356 nm and the sample emission were performed until 1-2 × 10^4 counts at the maximum were reached. The fluorescence decays were analyzed using the modulating functions method of Striker with automatic correction for the photomultiplier "wavelength shift" [34]. The method used to determine the fluorescence quantum yields of compounds **3a-d** (Φ_F^C) involve a connection between the fluorescence quantum yield of a reference (Φ_F^{ref}) and Φ_F^C. Anthracene was the reference used (Φ_F^{ref} = 0.27, in ethanol (EtOH), [35]). Firstly absorbance of the reference, in EtOH, and compounds, in DMSO, were adjusted to similar values (below 0.10) at the excitation wavelength. After this, the fluorescence spectra were recorded, under identical experimental conditions, and a comparison was made between the integrated areas under the fluorescence spectra of both the reference and the compounds. At last the **Equation (4)** was followed in order to obtain the Φ_F^C values [35], where A_{ref} and A_C are respectively the

$$\Phi_F^C = [(A_{ref}\, F_C\, n^2_C)/(\, A_C\, F_{ref}\, n^2_{ref})]\, \Phi_F^{ref} \quad \textbf{(4)}$$

absorbance of reference and compounds at the excitation wavelength, F_C is the integrated emission area of the compounds ($\int I(\lambda)^C\, d\lambda$) and F_{ref} is the integrated emission area of the reference spectra ($\int I(\lambda)^{ref}\, d\lambda$), n_C and n_{ref} are respectively the refraction index of the solvent containing the compound (DMSO), n_{DMSO} =1.4793 and the reference (EtOH), n_{DMSO} =1.3611. [27]

Synthesis:

9-Aminomethyl anthracene, **1** (0.1 g, $4.83x10^{-4}$mol) was dissolved in ca. 5 mL of freshly distilled dry CH_2Cl_2. To this solution 1.1 equivalent of the appropriate isocyanate in a single portion was added. Off-white or light yellow precipitates were immediately formed upon addition of the isocyanate. The reaction was allowed to stir for several hours, before the precipitate was isolated by filtration, washed with dry CH_2Cl_2 and dried under high vacuum (over P_2O_5) and eventually recrystallised from $CHCl_3$ to give powders.

1-Anthracen-9-ylmethyl-3-(2,4-difluoro-phenyl)-urea (3a)

Was obtained as an off-white solid in 80% yield. MS (ES^+) m/z = 385.11 [M + Na]. Calculated for $C_{22}H_{16}N_2OF_2Na$ [M+Na] m/z = 385.1128. Found m/z = 385.1111. Anal.Calcd for $C_{22}H_{16}N_2OF_2$: C, 72.92; H, 4.45; N, 7.73; Found: C, 72.67; H, 4.45; N, 7.62%. ^{1}H-NMR (400 MHz, DMSO-d_6): δ_H, 8.63 (s, 1H, AnthrCH), 8.47 (s, 1H, NH), 8.45 (s, 1H, NH), 8.18 (m, 4H, ArCH), 8.12 (s, 2H, AnthrCH), 7.64 (t, 2H, AnthrCH, *J* = 8 Hz), 7.56 (t, 2H, AnthrCH, *J* = 8.04 Hz), 7.21 (m, 1H, ArCH), 7.10 (m, 1H, AnthrCH), 7.02 (t, 1H, ArCH, *J* = 9.04 Hz), 5.33 (d, 2H, CH_2, *J* = 5 Hz); ^{13}C- NMR (100 MHz, $CDCl_3$): δ_C, 154.61, 152.59, 150.05, 131.09, 130.38, 129.69, 128.99, 127.37, 126.49, 125.30, 124.86, 124.82, 124.72, 124.28, 120.98, 120.89, 110.99, 110.78, 103.79, 103.52, 103.29, 35.15.

1-Anthracen-9-ylmethyl-3-tolyl-urea (3b)

Was obtained as an off-white solid in 84% yield, mp 215-218^{o}C; Calculated for $C_{17}H_{16}N_2S$:C, 72.82%; H, 5.75%; N, 9.99%; Found C, 70.01%; H, 4.30%; N, 7.05%; ^{1}H-NMR (400 MHz, $CDCl_3$): δ_H, 8.68 (s, 1H, Ar-10H), 8.64 (s, 2H, Ar-4H, Ar-5H), 8.49 (d, 2H, *J* = 9.0 Hz, Ar-1H, Ar-8H), 8.15 (d, 2H, *J* = 8.5 Hz, Ar-3H, Ar-6H), 7.65 (q, 2H, J_1 = 6.5 Hz, J_2 = 7.5 Hz, Ar-18H, Ar-22H), 7.56 (d, 2H, *J* = 7.0 Hz, Ar-3H, Ar-6H), 5.35 (s, 2H, 15-H, *J* = 3 Hz); ^{13}C- NMR (100 MHz, $CDCl_3$): δ_C, 160, 138.57, 131.85, 131.29, 130.55,

129.76, 128.88, 128.76, 126.99, 125.32, 125.08, 124.01, 123.92, 120.50, 57.43; ^{19}F NMR: 66.96; IR (KBr) cm^{-1} 3427, 3342, 2922, 1641, 1550, 1330, 729.

1-Anthracen-9-ylmethyl-3-(3,5-dimethyl-phenyl)-urea (3c)

Was obtained as an off-white solid in 80% yield. MS (ES$^+$) m/z = 377.16 [M + Na]. Calculated for $C_{24}H_{22}N_2ONa$ [M+Na] m/z = 377.1630. Found m/z = 377.1637. Calculated for $C_{24}H_{22}N_2O$: C, 81.33; H, 6.26; N, 7.90; Found: C, 80.63; H, 6.11; N, 7.81%. ^{1}H-NMR (400 MHz, DMSO-d_6): δ_H, 8.62 (s, 1H, AnthrCH), 8.47 (d, 2H, AnthrCH, *J* = 9.04 Hz), 8. 14 (s, 1H, NH), 8.12 (s, 2H, AnthrCH), 7.63 (t, 2H, AnthrCH, *J* = 9.04 Hz), 7.55 (t, 2H, AnthrCH, *J* = 8.04 Hz), 6.99 (s, 2H, ArCH), 6.61 (s, 1H, NH), 6.54 (s, 1H, ArCH), 5.30 (d, 2H, CH_2, *J* = 5 Hz), 2.19 (s, 6H, CH_3); ^{13}C-NMR (100 MHz, $CDCl_3$): δ_C, 171.74, 170.39, 170.20, 162.40, 145.05, 142.18, 123.88, 119.03, 57.29, 54.63, 54.52, 53.04, 36.30, 35.77, 35.65, 35.23, 35.14, 35.08.

1-Anthracen-9-ylmethyl-3-phenyl-urea (3d)

Was obtained as an off-white solid 77% yield. mp 209-210^{o}C; Calculated for $C_{22}H_{17}N_2O$:C, 80.96%; H, 5.56%; N, 8.58%; found C, 80.96%; H, 5.55%; N, 8.59%; ^{1}H-NMR (400 MHz, DMSO-d_6): δ_H, 8.15 (s, 1H, Ar-10H), 7.96(d, 2H, *J* = 9.0 Hz, Ar-1H, Ar-8H), 7.89 (s, 2H, , Ar-4H, Ar-5H), 7.64 (s, 2H, Ar-18H, Ar-22H), 7.38 (d, 2H, *J* = 9.0 Hz, Ar-2H, Ar-7H), 7.37(d, 2H, *J* = 8.0 Hz, Ar-3H, Ar-6H), 7.24 (s, 2H, Ar-19H, Ar-21H), 7.09 (s, 1H, Ar-20H), 4.86 (s, 2H, Ar-15H); ^{13}C-NMR (100 MHz, $CDCl_3$): δ_C, 160, 138.53, 131.91, 131.26, 130.56, 129.76, 128.94, 128.67, 126.81, 125.35, 125.06, 124.01, 123.92, 120.50, 54.41.

References:

[1] J. F. Callan, A.P. de Silva, D.C. Magri, *Tetrahedron,* **2005**, *36*, 8551; See special issue on Fluorescent Sensors: *J. Mater. Chem*., **2005**, *15*, 2617-2976.

[2] deSilva, A.P.; Gunaratne, H.Q.N.; Gunnlaugsson, T.; Huxley, A. J. M.; McCoy, C. P.; Rademacher J. T.; Rice, T. E. *Chem. Rev*. **1997**, *97*, 1515.

[3] Gunnlaugsson, T.; Leonard J.P. *Chem. Commun*. **2005**, 3114. (b) Leonard J.P.; Gunnlaugsson T. *J. of. Fluoresc.* **2005**, *15*, 585.

[4] Sessler, J. L.; Gale, P. A.; Cho, W. S., *Anion Receptor Chemistry*; Royal Society of Chemistry: Cambridge, UK.

[5] Steed, J. W., *Chem. Commun*., **2006**, 2637; Martínez-Máñez, R. Sancenón, F. *Chem. Rev*, **2003**, *103*, 4419. Suksai, C.; Tuntulani, T. *Chem. Soc. Rev*., **2003**, *32***,** 192.

[6] Gale, P.A. *Coord. Chem. Rev.,* **2001**, *213*, 79; Gale, P.A. *Coord. Chem. Rev.,* **2000**, *199*, 181; Beer P.D.; Gale, P.A. *Angew. Chem. Int. Ed.,* **2001**, *40*, 486.

[7] Gale, P. A., *Acc. Chem. Res*., **2006**, *39*, 465. Gale P. A. *Chem. Commun*., **2005**, 3761.

[8] Matthews, S. E.; Beer, P. D., *Supramol. Chem*., **2005**, *17*, 411; Davis A. P., Joos J. B., *Coord. Chem. Rev*., **2003**, ***240*,** 143.

[9] Gunnlaugsson, T.; Glynn, M.; Tocci (née Hussey), G. M.; Kruger, P. E.; Pfeffer, F. M. *Coord. Chem. Rev*., **2006**, *250*, 3094; Gunnlaugsson, T.; Ali H.D.P.; Glynn, M.; Kruger, P.E.; Hussey G. M. Pfeffer F. M.; dos Santos, C. M. G.; Tierney, J.; *J. of. Fluoresc.*, **2005**, *15,* 287.

[10] Bianchi, E. Bowman-James, K. García-España, E. Eds. *Supramolecular Chemistry of Anions*, Wiley-VCH, New York, 1997.

[11] Light, M.E.; Gale, P.A.; Navakhun, K.; Quesada, R. *Chem. Commun.*, **2006**, 901; Brooks, S. J.; Edwards, P. R.; Gale, P. A.; Light, M. E. *New. J. Chem*. **2006**, *30*, 65; Brooks, S. J.; Gale, P. A.; Light, M. E. *Chem. Commun.* **2005**, 4696.

[12] Brooks, S. J.; Gale, P. A.; Light, M. E. *Chem. Commun.* **2006**, 4344.

[13] Pfeffer, F. M,; Seter, M.; Lewcenko, N.; Barnett, N. W. *Tetrahedron Lett.,* **2006**, *47*, 5241; Pfeffer F. M.; Buschgens, A. M.; Barnett, N. W.; Gunnlaugsson, T.; Kruger, P. E., *Tetrahedron Lett.,* **2005**, *46*, 6579; Pfeffer, F. M.; Gunnlaugsson, T.; Jensen, P.; Kruger, P.E., *Org. Lett*. **2005**, *7*, 5375.

[14] Wel L. H.; He, Y. B.; Wu, J. L.; Wu, X. J.; Meng, L., Yang, X. *Supramol. Chem.,* **2004**, *16*, 561.

[15] Gómez D. E., Fabbrizzi, L., Licchelli, M., Monzani, E. *Org. Biomol. Chem*., **2005**, *3*, 1495; Boiocchi, M.; Boca, L.D.; Gómez, D.E.; Fabbrizzi, L.; Licchelli, M.; Monzani, E. *J. Am. Chem. Soc.*, **2004**, *126*, 16507.

[16] Wu, F.Y.; Li, Z.; Gua, L.; Wang, X.; Lin, M.H.; Zhao, Y.F.; Jiang, J.B. *Org. Biomol. Chem*. **2006**, *4*, 624; Wen, Z.C.; Jiang, Y.B. *Tetrahedron,* **2004**, *60*,11109; Wu, F.Y.; Li, Z.; Wen, Z.C.; Zhou, N.; Zhao, Y.F.; Jiang, Y.B. *Org. Lett*., **2002**, *4*, 3202.

[17] Gunnlaugsson, T.; Davis, A.P.; Glynn, M. *Chem. Commun*., **2001**, 2556; Gunnlaugsson, T. Davis, A.P. Hussey, G. M. Tierney, J. Glynn, M. *Org. Biomol. Chem*., **2004**, *2*, 1856; Gunnlaugsson, T.; Davis, A. P.; O'Brien, J. E.; Glynn M., *Organic Lett.* **2002**, *4*, 2449; Gunnlaugsson, T.; Davis, A. P.; O'Brien, J. E.; Glynn, M. *Org. Biomol. Chem.*, **2005**, *3,* 48.

[18] Quinlan E.; Matthews S. E.; Gunnlaugsson, T., *Tetrahedron Lett.,* **2006**, *47*, 9333.

[19] Gunnlaugsson, T.; Kruger, P. E.; Lee, T. C.; Parkesh, R.; Pfeffer, F. M.; Hussey**,** G. M.; *Tetrahedron Lett.*, **2003**, *44*, 6575.

[20] Harte, A. J.; Jensen, P.; Plush, S. E.; Kruger, P. E.; Gunnlaugsson, T.; *Inorg. Chem.* **2006**, *45*, 9465; Gunnlaugsson, T.; Harte, A. J.; Leonard, J. P.; Nieuwenhuyzen, M. *Supramol. Chem.* **2003**, *15*, 505; Gunnlaugsson, T.; Harte, A. J.; Leonard, J. P.; Nieuwenhuyzen, M. *Chem. Commun.* **2002**, 2134.

[21] Leonard, J. P.; dos Santos, C. M. G.; Plush, S. E.; McCabe, T., Gunnlaugsson, T. *Chem. Commun*., **2006**, **DOI:** 10.1039/b611487c

[22] Parkesh, R.; Lee, T. C.; Gunnlaugsson, T. *Org. Biomol. Chem*., **2007**, *5*, 310; Gunnlaugsson, T.; Leonard J. P.; Murrey, N.S. *Organic. Lett*, **2004**, 6, 1557; Gunnlaugsson, T.; Harte, A. J.; Leonard J. P.; Senegal, K. *Chem. Commun.*, **2004**, 782; Gunnlaugsson, T.; Lee C. T.; Parkesh, R. *Organic. Lett*, **2003**, *5*, 4065; Gunnlaugsson, T.; Lee, T. C.; Parkesh, R. *Org. Biomol. Chem*., **2003**, *1*, 3265; Gunnlaugsson, T.; Bichell, B.; Nolan, C. *Tetrahedron Lett*., **2002**, *43*, 4989; Gunnlaugsson, T.; Nieuwenhuyzen, M.; Ludovic R.; Vera T. *Tetrahedron Lett.,*, **2001,** *42***,** 4725; de Silva, A. P.; Gunaratne, H. Q. N.; Gunnlaugsson, T.; Nieuwenhuyzen, M. *Chem. Commun.*, **1996**, 1967.

[23] The data were collected on a Bruker Smart Apex Diffractometer*. The crystal was mounted on 0.35mm quartz fibre and immediately placed on the goniometer head in a 123K N2 gas stream. The data was acquired using Smart Version 5.625 software in multi-run mode and 2400 frames in total, at 0.3^{o} per frame, were collected. Data integration and reduction was carried out using Bruker Saint+ Version 6.45 software and corrected for absorption and polarization effects using Sadabs Version 2.10 software. Space group determination, structure solution and refinement were obtained using Bruker Shelxtl Ver. 6.14 software. SMART Software Reference Manual, version 5.625, Bruker Analytical X-Ray Systems Inc., Madison, WI, 2001. Sheldrick, G. M. SHELXTL, An Integrated System for Data Collection, Processing, Structure Solution and Refinement, Bruker Analytical X-Ray Systems Inc., Madison, WI, 2001.

[24] ***Crystal data*:-** C25 H23 F3 N2 O2 S, Monoclinic, space group C2/c, a = 31.430(3), b = 8.7283(9), c = 16.3151(17) Å, β = 97.952(2)^{o}, U = 4432.6(8) Å^{3}, T = 123 K, μ (Mo–Kα) = 0.191mm^{-1}, Z = 8, A total of 14403 reflections were measured for 4 < 2Θ <57 and 3169 unique reflections were used in the refinement, [R(int) = 0.0391], the final parameters were wR2 = 0.1102 and R1 = 0.0466[I>2σ(I)]. CCDC 627537.

[25] Bouas-Laurent, H.; Castellan, A., Desvergne, J.-P.; Lapouyade, R. *Chem. Soc, Rev.,* **2001**, *30*, 248; Bouas-Laurent, H.; Castellan, A., Desvergne, J.-P.; Lapouyade, R. *Chem. Soc, Rev.,* **2000**, *29*, 43.

[26] Molard, Y.; Bassani, D. M.; Desvergne, J.-P.; Moran, N.; Tucker, J. H. R. *J. Org. Chem.,* **2006**, *71*, 8523.

[27] Murov, S. L.; Carmichael, I.; Hug, G. L. *Handbook of Photochemistry*, 2nd ed.; Marcel Dekker, Inc.: New York, 1993.

[28] Martell, A. E.; Motekaitis, R. J. *The determination and use of stability constants*; VCH Publishers: Weinheim, 1988.

[29] Gunnlaugsson, T.; Kruger, P.E.; Jensen, P.; Pfeffer, F. M.; Hussey, G. M. *Tetrahedron Lett.*, **2003**, *44* 8909.

[30] Kang, S.O.; Powell, D.; Day, V.W.; Bowman-James, K. *Angew. Chem. Int. Ed.*, **2006**, *45*, 1921.

[31] Lordeiro, C.; Pina, F.; Parola, A. J.; Bencini, A.; Bianchi, A.; Bazzicalupi, C.; Ciattini, S.; Giorgi, C.; Masotti, A.; Valtancoli, B.; Seixas de Melo, J. *Inorg. Chem.*, **2001**, *40*, 6813; Amire, S. A; Burrows, H. D.; *J. Chem. Soc., Faraday Trans. 1*, **1982**, *78*, 2033; Rehm, D.; Weller, A. *Israel J. Chem.*, **1970,** *8*, 259 – 271.

[32] Seixas de Melo, J.; Silva, L. M.; Kuroda, M. *J. Chem. Phys.*, **2001,** *115*, 5625.

[33] Seixas de Melo, J.; Fernandes, P. F. *J. Mol. Struct.*, **2001,** *565 – 566*, 69.

[34] Stricker, G.; Subramaniam, V.; Seidel, C. A. M.; Volkmer, A. *J. Phys. Chem. B*, **1999**, *103*. 8612.

[35] Ramachandram, B.; Samanta, A. *Chem. Phys. Let.*, **1998,** *290*, 9.

Synthesis, Structural and Photophysical Evaluations of Urea based Fluorescent PET Sensors for Anions

Cidália M. G. dos Santos,[a,b] Mark Glynn,[a] Tomas McCabe,[a] J. Sérgio Seixas de Melo,[b] Hugh D. Burrows[b] and Thorfinnur Gunnlaugsson[a*]

a) School of Chemistry, Centre for Synthesis and Chemical Biology, Trinity College Dublin, Dublin 2, Ireland.

b) Departamento de Química, Faculdade de Ciências e Tecnologia, Universidade de Coimbra, Portugal.

Abstract: The design, synthesis and photophysical evaluation of four anthracene based photoinduced electron transfer (PET) sensors (**3a-d**) for anions is described. The [4π+4π] photodimerization product, **4**, was also obtained from **3b**, by slow evaporation from DMSO solution and its X-ray crystal structure determined. The structure of **4**, showed the classical dimerization at the 9,10-positions of anthracene. Sensors **3a-d** are all based on the use of charge neutral aryl urea receptors, where the recognition of anions such as acetate, phosphate and iodide, was found to be due to the formation of strong hydrogen bonding interactions in DMSO. This anion recognition resulted in enhanced quenching of the anthracene excited state *via* electron transfer from the receptor; hence the emission was '*switched on-off*'. The sensing of fluoride was, however, found to be a two-step process, which involved initial hydrogen bonding interactions with the receptor, followed by deprotonation and the formation of bifluoride (HF_2^-). The changes in the emission spectra upon sensing of chloride and bromide were, however, minor. The photophysical properties of these sensors in the presence of various anions were further studied, including investigation of their excited state lifetimes and

* Corresponding author. Phone: +353 1 896 3459. Fax: +353 1 671 2826. E-mail: gunnlaut@tcd.ie

quantum yields, as well as detailed Stern-Volmer kinetic analysis with the aim of determining the dynamic and static quenching constants, k_q and k_s for the above anion recognition. These measurements indicated that while the anion dependant quenching was mostly by a dynamic process, some contribution from static quenching was also observed at lower anion concentrations.

INTRODUCTION

Over the years, much effort has been devoted to the development of selective and sensitive optical chemosensors for real time detection of ions and molecules which are of major interest in clinical analysis and diagnostics, biology and environmental chemistry.[1-3] The sensing of anions has become an important area of research in supramolecular chemistry, with many excellent examples being published in the last few years.[4-6] Particular emphasis has been placed on the use of charge neutral anion receptors such as thioureas, ureas and amidoureas, as well as amides and pyrroles as anion recognition moieties. The incorporation of these into chromophores and fluorophores with the aim of developing colorimetric and fluorescent sensors for anions has become an important area of research.[7-10] Gale *et al.* have been at the forefront of such research and have recently used anion binding motifs such as amidoureas in naked eye detection of biologically important anions, by incorporating these binding moieties as integrated parts of 'push-pull' chromophores, as well as including such anion recognition sites into macrocyclic structures.[11,12] Several other groups, such as Pfeiffer *et al.*[13], He *et al.* [14], Fabbrizzi *et al.*[15] and Jiang *et al.* [16] have also used similar aryl based ureas or thiourea architectures to achieve colorimetric sensing of anions. At the same time, we developed the first examples of charge neutral PET sensors for anions using thiourea receptors.[17] We have also developed sensors using aminourea based receptors for the recognition of anions in aqueous solution, or by incorporating such binding

motifs into preorganized structural scaffolds such as calix[4]arene.[18] We have also demonstrated the fixation of CO_2 as HCO_2^- by using colorimetric anion sensors based on the naphthalimide fluorophore,[19] and have shown that lanthanide (Tb(III) or Eu(III)) luminescent complexes can be employed to detect aromatic or aliphatic mono and bis-carboxylates in competitive media, or by using displacement assays. [20,21]

In our earlier work, which was centred on developing charge neutral fluorescent anion sensors, we focused on the use of anthracene and naphthalimide based sensors, where the changes in the fluorescence intensity of these sensors were monitored upon increased anion concentration.[17,19] We showed that the recognition of these anions, on all occasions, gave rise to reduced emission, which we describe as an '*on-off*' emission changes. We proposed that these changes were due to enhanced photoinduced electron transfer (PET) quenching of the fluorophore excited state from the anion receptor, upon anion recognition. However, a more comprehensive photophysical investigation into this phenomenon has not been carried out in our laboratory, and with this in mind we set out to develop several new fluorescent PET sensors using substituted urea receptors. These sensors, **3a-3d**, are all based on the classical *fluorophore-spacer-receptor* model, where the aryl receptor is separated from the flourophore fluorophore by a short spacer.[22] These are also the first examples of such urea based sensors from our laboratory.

The urea receptors, **3a-3d**, were also selected in such a manner to gain further insight into the effect that the aryl based receptors would have on: *a*) the binding affinity of the receptor and *b*) the efficiency of the electron transfer quenching. Hence, questions such as do the more electron withdrawing receptors give rise to stronger binding and hence more efficient quenching than electron donating ones (as such inductive effects would make the urea protons more acidic and hence, stronger hydrogen bonding donors), had not been fully answered. Herein, we give a full account of our investigation, which involved the titration of

3a-3d with various anions and observing the changes in the various photophysical properties of these compounds upon anion sensing.

RESULTS AND DISCUSSION

Synthesis of compounds 3a-3d

The synthesis of the desired urea based sensors was achieved in high yield in a single step, Scheme 1, from 9-aminomethyl anthracene, **1**, by reacting it with the commercially available isocyanides: 2,4-difluorophenyl-,(**2a**), 4-(trifluoromethyl) phenyl-,(**2b**), 3,5-dimethylphenyl-

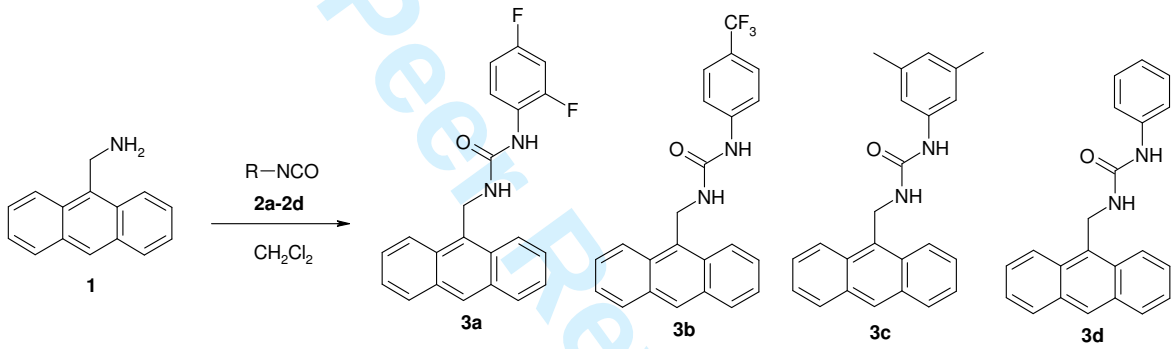

Scheme 1. Synthesis of the urea based anion sensors **3a-3d**. See text for **2a-2d**.

(**2c**) and phenyl- isocyanate, (**2d**), respectively, in dry CH_2Cl_2, at room temperature. In all cases, upon addition of **2a-d** to **1**, creamy pale yellow precipitates were immediately observed. Nevertheless, the reactions were left stirring overnight. The resulting precipitates were then collected by suction filtration, washed several times with cold CH_2Cl_2 and dried under high vacuum. Compounds **3a-d** were all obtained in yields of 80-97% after recrystallisation from $CHCl_3$. All the compounds were characterised using conventional methods (see experimental section). The sensors were partially soluble in $CDCl_3$, and fully soluble in DMSO-d_6. In the latter solvent, two characteristic resonances were observed at 8.47 ppm and 8.45 ppm, for the urea protons of the electron deficient **3a**, while for the electron rich sensor **3d** these protons apperad at 8. 14 ppm and 6.61 ppm.

The X-ray crystal structure analysis of [2+2] photochemical adduct of 3b

Several attempts were made to obtain crystals of the above sensors for X-ray crystal structure analysis. However, the use of slow evaporation or diffusion techniques failed on all occasions. In contrast, colourless crystals were obtained from an NMR sample of **3b**, in DMSO-d_6, and were found to be suitable for X-ray crystal structure analysis.[23,24] Although, to our

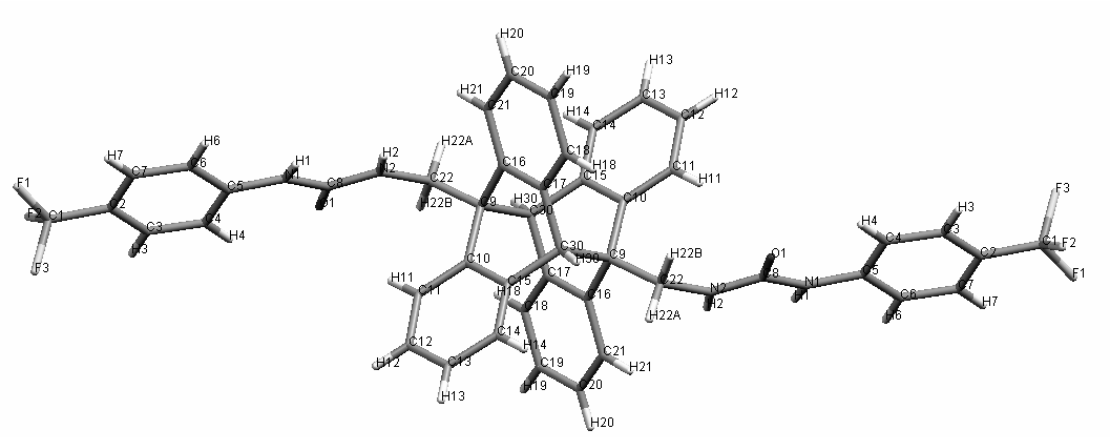

Figure 1. The X-ray crystal structure of the [4π+4π] cyclcoaddition product **4**, formed from **3b**. A DMSO molecule has been removed for clarity (see text).

surprise, the structure was not that of the desired sensor **3b**, but the product of the resulting [4π+4π] photocycloaddition dimerization reaction between two molecules of **3b**, *i.e.* **4**. The new bonds were formed between the central rings on each anthracene unit as is evident from Figure 1. It also shows that the structure adopts C_2 symmetry with the two urea receptors being *anti* to each other, with a single DMSO molecule being found in the unit cell. This structure can only be obtained photochemically, which is however, thermally reversible, and only from the desired compound **3b**. Hence, **4** can be viewed as being the proof of the formation of **3b**. This photochemical reaction is a common phenomenon for anthracene, which can be dimerized easily upon UV radiation.[25,26] However, the sample that these crystals were grown from was only exposed to halogen based room-light and/or sunlight. We therefore propose that the urea receptor activates the 9 position of the anthracene sensor **3b** in such a way that it dimerizes in this manner. The structure of **4**, is one of two possible structural isomers; the other being where the two receptors would be on the same side ('*syn*'

to each other) of the photodimerised product of **3b**. This is also known as the *head-to-tail* product.[25,26] Compound **4**, is however, the so called tail-to-tail product, and is described as being the more stable of the two isomers. It is usually the product isolated upon photodimerization of such 9-substituted anthracene molecules. This is also believed to be the more thermally reversible product. As is typical for such dimerization products, the four aryl rings adopt a double wing like appearance, with a C…C bond length of 1.626(4) Å between the two former anthracene 9 and 10 positions. Moreover, the bond angle between the C9-C30-C17 atoms was found to be on average 113.1°, which is also typical for such products. The structure also shows that the urea moieties are almost coplanar with the 4-(trifluoromethyl) phenyl groups, with average N…H bond length of 0.860Å.

The packing diagram of **4** viewed down the crystallographic c axes can be seen in Figure 2. This shows that each of the urea moieties is hydrogen bonded to the oxygen of an aforementioned DMSO molecule, with a O…H bond length of 2.95 Å. However, even

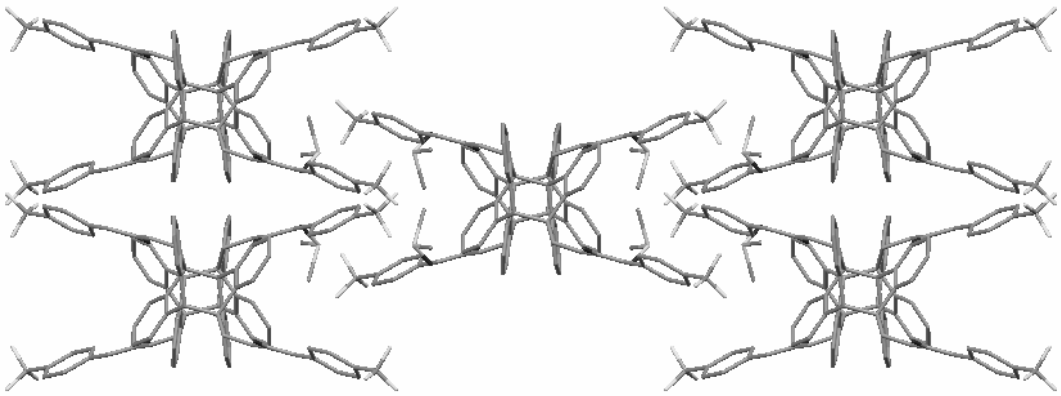

Figure 2. The packing diagram for **4** by viewing down the c-axis. Hydrogen atoms and short-contacts have been removed for clarity.

though the 4-(trifluoromethyl) phenyl groups show evidence of stacking, the distance between the two aryl groups is 8.7Å, which is too long to account for any π–π stacking interactions. There is however, a further F…H interaction between the aryl CF_3 groups and the protons of

the DMSO molecules with average F…H distance of 2.66 Å. The anion recognition ability of this structure was not evaluated.

Photophysical evaluation of 3a-3d

The photophysical properties of the four sensors were evaluated in DMSO. The ground state properties of **3a-3d** were first investigated. The absorption spectra of all the sensors were almost identical, when recorded in DMSO, with bands appearing at 340, 369 and 324 nm, respectively, and a shoulder at 333 nm which was assigned to the aryl groups of the receptor moieties. These are significantly shifted towards the red in comparison with anthracene, which has three characteristic bands appearing at 342, 360 and 380 nm, respectively.[27] For these four sensors, extinction coefficients of 9920, 10830, 7279 and 9560 [$Mol^{-1}cm^{-1}$] were determined in DMSO for **3a-3d**, respectively.

Using for excitation, the 369 nm transition of the anthracene based sensors, and the 360 nm band of the reference anthracene chromophore, the fluorescence emission spectra were recorded in DMSO. Here, the characteristic fluorescence emission of the anthracene fluorophore was observed for all the compounds, with that of the sensors being red-shifted by

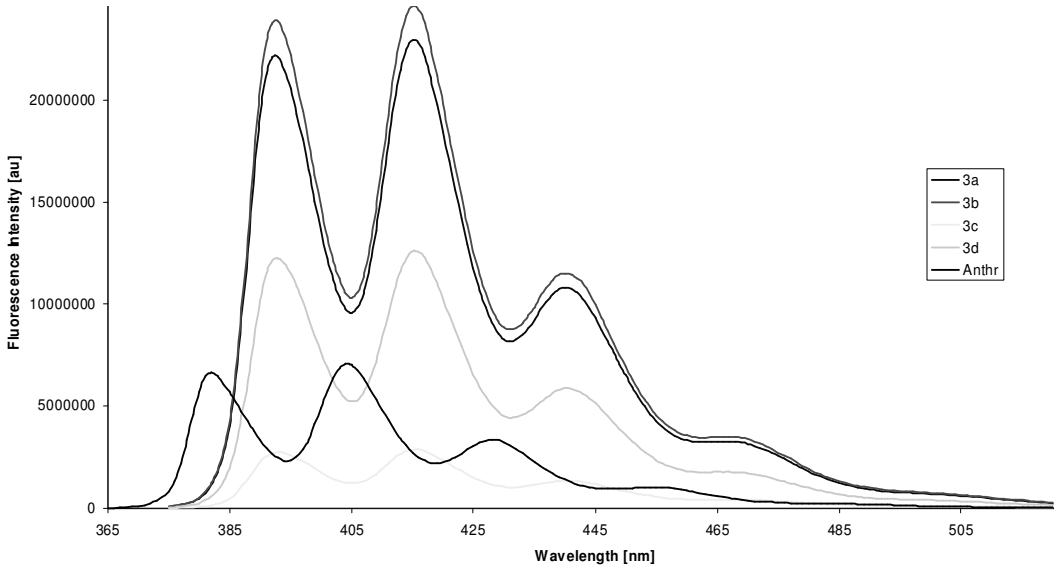

Figure 3. Comparison between the fluorescence emission spectra of chemosensors **3a-d** and the spectrum of anthracene, **Anthr**, in DMSO.

ca. 10 nm in comparison with that of anthracene itself, Figure 3, emitting at 393, 415 and 440 nm, with a shoulder at 466 nm. As can be seen from Figure 3, the intensity of all the sensors, with the exception of **3c**, was greater than that of the reference anthracene compound. For **3a-3d** the quantum yields of fluorescence (Φ_F) were determined as 0.53, 0.57, 0.06 and 0.33, respectively under these experimental conditions, where the order is **3a>3b>3d>3c**, which shows that the more electron withdrawing substituents give rise to the higher quantum yields. This follows a known trend, where 9,10-dimethyl anthracene has a higher quantum yield than 9-methyl-anthrancene, which subsequently has higher quantum yield than anthracene itself. However, and perhaps somewhat surprising, then it is worth noting that in the case of **3c**, the di-substitution at the aryl ring gives rise to a very low quantum yield in comparison the rest of the sensors. A similar trend was seen for the fluorescence lifetimes (τ_F) in DMSO. The decays upon excitation of the 356 nm transition and observation at 450 nm were all single exponential, and had lifetimes 7.83, 8.99, 1.32 and 4.96 ns, respectively for the sensors **3a-3d.** From these changes, the rate constants for fluorescence k_F, can be determined, as being 6.76×10^7, 6.34×10^7, 4.55×10^7 and $6.67\times10^7 s^{-1}$ for **3a-3d**, respectively. From these results it is clear, that even though there is no significant difference in either the λ_{Absmax} or λ_{Fmax} for these sensors, the anion urea receptors have a significant effect on both Φ_F and τ_F. This is most pronounced for the electron rich reporter system **3c**, where Φ_F and τ_F are significantly lower than that observed for the remaining sensors. This is most likely to be due to a more efficient photoinduced electron transfer quenching of the anthracene excited state by **3c**, in its 'free' form (in the absence of any anions), while the electron withdrawing substituents of **3a** and **3b** make the aromatic urea electron deficient and hence less able to participate in PET quenching. This is supported by the fact that the results obtained for sensor **3d**, follow this trend, where both the Φ_F and τ_F are smaller than that of **3a** and **3b**, but larger than that of **3c**. It is also

worth noting that **3a** and **3b**, which have electron withdrawing substituents on their receptors, seem to have very similar photophysical properties.

Anion binding evaluations of compounds 3a-3d

Having established the fundamental photophysical properties of compounds **3a-3d**, the four compounds synthesised above were evaluated for their ability to detect anions in DMSO, by observing the changes in both the absorption and fluorescence emission spectra upon titrating these sensors with stock solutions of AcO^-, $H_2PO_4^-$, F^-, Cl^-, Br^- and I^- (as their tetrabutyl ammonium salts). Upon titration of these sensors with anions such as AcO^-, $H_2PO_4^-$, F^-, only minor changes were seen in the absorption spectra for the anthracene component at longer wavelengths, while more significant changes were seen at shorter wavelengths. While

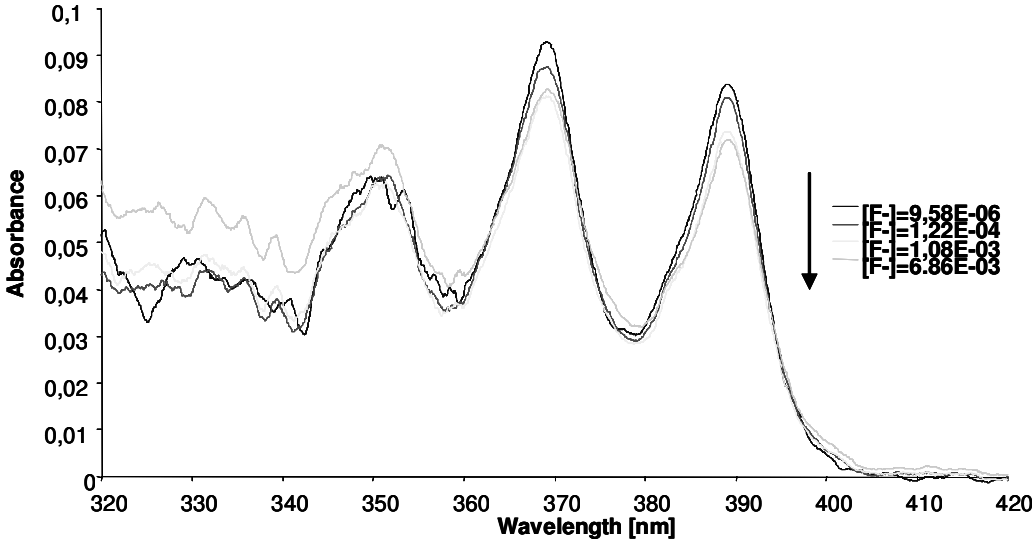

Figure 4. The changes in the absorption spectra of **3a** upon titration with F^- upon excitation of 369 nm, in DMSO.

these latter changes were assigned to the interaction of the anion at the urea receptor, the lack of changes in the anthracene transitions is not all together surprising as the methylene spacer should prevent any significant ground state interactions between the two parts. This is clear from Figure 4 which shows the titration of **3a** with F^-, where the major changes in the

absorption spectra occur at short wavelengths, indicating direct interaction between the receptor and the anion through hydrogen bonding.

Similar results were observed for $H_2PO_4^-$. When these measurements were made using AcO^- the changes in the shorter wavelengths were more pronounced. In comparison to these changes, the absorption spectra of **3a-3d** were not affected by the addition of either Cl^- or Br^-. However, upon titration of these sensors with I^- no significant changes were observed in the absorption spectra at low and medium concentrations (0→ 3 mM), while at high concentrations (~ 0.02M) the fine structure of the absorption spectra was displaced by an intense, broad structure, signifying strong ground state interactions between these sensors and I^- under these conditions. In general, the changes in the absorption spectra of the fluorophore, with the exception of I^- can be considered to be minor and only the changes at short wavelengths, assigned to that of the receptor are affected. This indicates that anions such as AcO^-, $H_2PO_4^-$, F^- only interact with the receptor part of the sensors and that the methylene spacer prevents any ground state interactions between the fluorophore and the receptor.

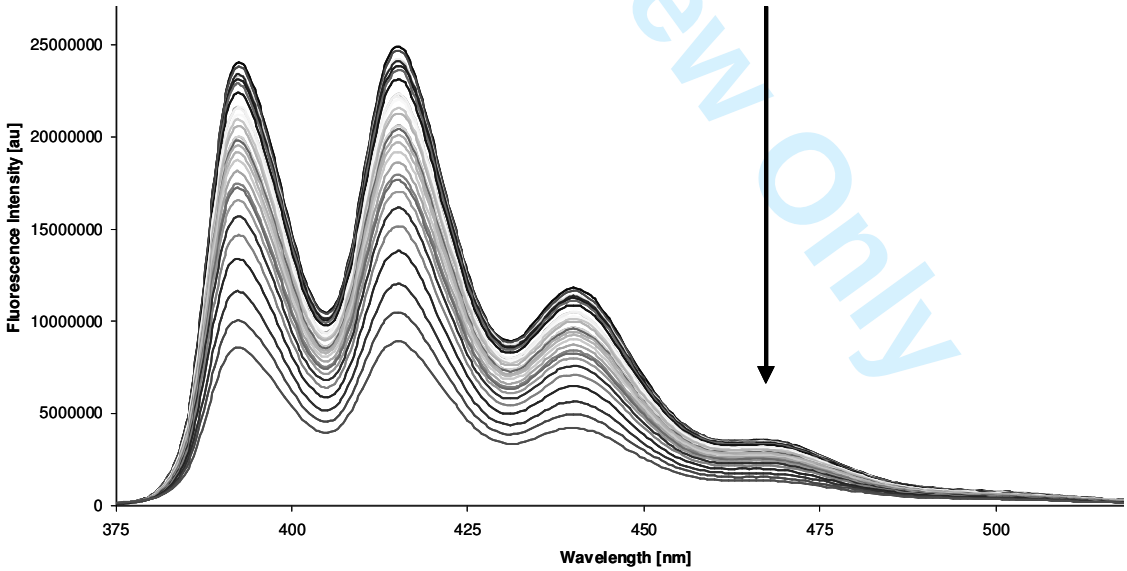

Figure 5. Fluorescence emission of **3a** titrated with TBAAcO, from top to bottom [AcO^-]= 0 to 6.27×10^{-2} M. From values of the fluorescence intensity at 415nm the value for the quenching extent was measured to be *ca.* 64%.

Hence, it can be concluded that these urea based sensors behave as 'ideal' PET sensors for anions.

In contrast to the changes in the absorption spectra, the anthracene based emission was significantly modulated upon titration with the above anions in DMSO. The changes observed for the titration of **3a** with AcO^-, is shown in Figures 5. It clearly demonstrates that the emission is quenched upon addition of AcO^-, signifying the recognition of the anion at the receptor side. It is also noticeable, that only the intensity of fluorescence is modulated and no significant changes are observed in the positions of the three characteristic anthracene emission bands. It can thus be concluded that these sensors behave as PET sensors, where the emission of the fluorophore is quenched by PET from the receptor to the excited sate of the fluorophore.

Unlike that observed for classical PET cation sensors, where the emission is enhanced due to the suppression of PET, caused by the increased oxidation potential of the receptor upon cation recognition, the emission here is reduced. This can be viewed as a result of the formation of a more electron rich anion-receptor complex, which gives rise to the enhancement of the reduction potential. As Figure 5 demonstrates, the changes in the emission spectra were homogenous across all the wavelengths, *i.e.* no particular transition was more reduced than the other. Consequently, by observing the changes in the 414 nm transition as a function of $\log[AcO^-]$, a sigmoidal plot was obtained, from which a binding constant $\log \beta$ was determined to be *ca.* 2. By plotting Log $[(I_{max}-I_F)/(I_F-I_{min})]$ as a function of $\log[AcO^-]$, a linear plot ($R^2 = 0.92$) was observed from which a $\log \beta = 2.14$ (±0.1) was determined.[28] This indicates a week binding between the sensor and the anion. When the same titrations were carried out using **3b-3d**, similar luminescent changes were observed, where the emission was quenched upon increasing anion concentration, without any measurable changes in λ_{max}. From these changes, binding constants of 2.44(±01), 2.07(±01) and 2.09(±01) were

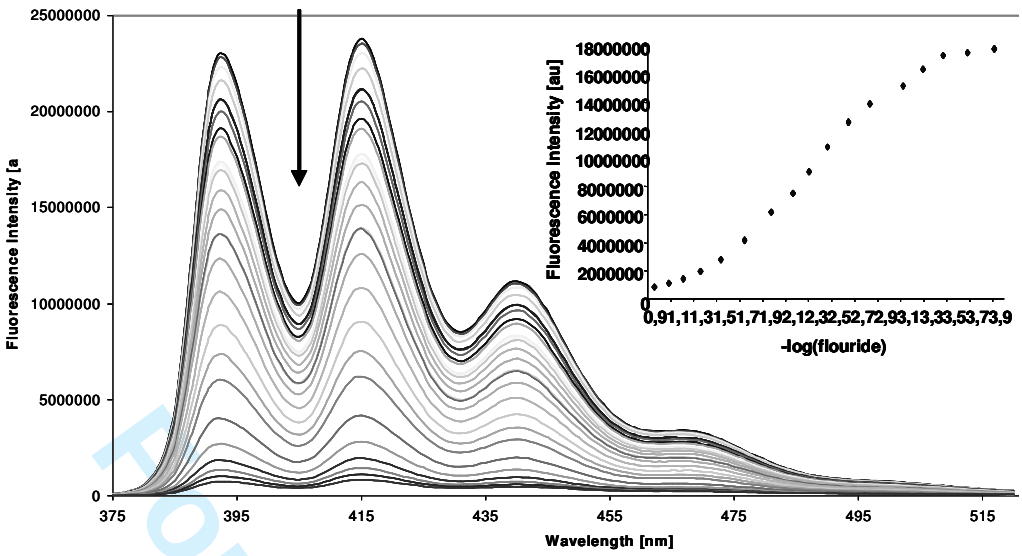

Figure 6. Fluorescence titration spectra showing the changes in fluorescence emission of **3a** in DMSO upon addition of fluoride, from top to bottom, $[F^-] = 0 \rightarrow 1.1\times10^{-1}$ M. Insert: The changes in the 415 nm transition as a function of $[F^-]$.

determined, for **3b-3d**, respectively. However, for all of these the quenching was more efficient than seen for **3a**, being 81%, 70% and 83% for these three sensors, respectively. The effect of the substituent on the aryl urea receptor can also be seen from these changes. However, these are not as dramatic as one would anticipate. While the binding affinity follows the trend of **3b>3a>3c ~3d**, displaying a marginally stronger binding for the two electron deficient receptors, there is no significant difference in these values. Hence, while the electron withdrawing groups would be expected to make the urea protons more acidic and as such, better hydrogen receptor, the difference in the binding constants does not reflect this. When these titrations were repeated using $H_2PO_4^-$, similar effects were observed. However, the degree of quenching was less, being 50%, 65%, 60% and 57% for the four sensors, respectively. From these changes binding constants (log β) of 1.91(±0.1), 2.11(±0.1), 1.90(±0.1), and 1.96(±0.1), were determined which follow the same trend as seen previously for acetate. When either Cl^- or Br^- were used, the emission was only partially quenched, and only at high concentrations. However, these changes were too small for accurate binding constant determination. We assign this quenching to the formation of a hydrogen bonding

complex between the anion and the receptor rather than being due to heavy atom affect quenching.

The titration of **3a-3d**, using F^- gave similar luminescent changes, *e.g.* no spectral shifts were observed and only the fluorescence emission was quenched, demonstrating effective PET quenching from the receptor upon anion recognition. However, unlike that seen above, the emission was almost fully quenched. This can be seen in Figure 6, for **3a**, which shows that the anthracene emission is reduced by almost 90% at the end of the titration. Similarly, the emission was quenched for **3b-3d**, where it was reduced by *ca*. 97%, 91% and 97%, respectively. From these changes, the binding constants log β of 2.73(±0.1), 3.26(±0.1), 2.59(±0.1) and 2.99(±0.1), were determined.

While the same trend is observed here as above, the binding constants as well as the efficiency of the quenching are significantly higher than seen for either AcO^- or $H_2PO_4^-$. We have previously postulated that this is due to two main phenomena. Firstly, the small ion has higher charge density than either AcO^- or $H_2PO_4^-$ and can form stronger hydrogen bonding complexes with the receptor. Secondly, F^- is a good base in DMSO.[27] Consequently, F^- can possibly deprotonate the urea receptor. This, has been shown to occur through a two step mechanism, which gives rise to the formation of bifluoride, HF_2^-, the formation of which can be monitored by NMR.[29] Moreover, the formation of such species in anion complexes has recently been demonstrated using X-ray crystallography.[30] This deprotonation results in the formation of a highly electron rich receptor, which consequently is also a more efficient PET quencher. It is also possible that the HF_2^- products form a very strong ground state complex with the receptor. With the aim of firmly establishing the nature of the quenching, we decided to determine the rate of the quenching process for all of the sensors using the aforementioned anions.

Kinetics of fluorescence quenching

In order to obtain the quenching rate constants, k_q, from fluorescence intensity measurements at different anion concentrations, [Q], the Stern-Volmer kinetics was followed, **Equation (1)**, where I_0 and I are the fluorescence emission in the absence of quencher (anion) and for a given concentration of anion [Q], respectively, K_{sv} and k_q are the Stern-Volmer and quenching rate constants respectively ($K_{sv} = k_q\ \tau_0$) and τ_0 is the lifetime in the absence of quencher.[27] Here the plot of I_0/I versus the anion concentration should be linear with a slope equal to $k_q\tau_0$. In Figure 7, the results for the titration of **3a** with F^- are shown. A

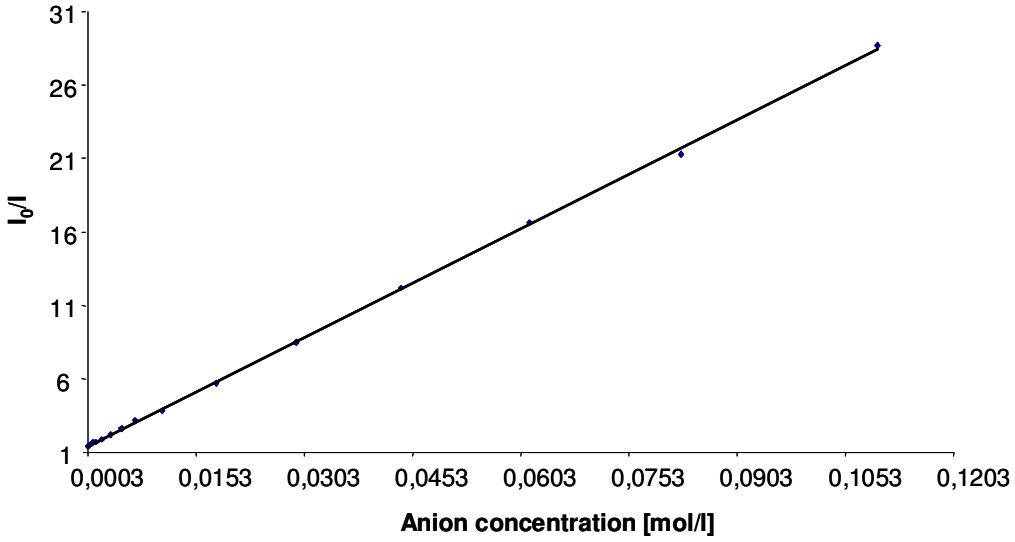

Figure 7. Stern-Volmer plot for the fluorescence quenching of **3a** by F^-. The solid line translates the theoretical curve from the Stern-Volmer **Equation (1)**.

quantitative analysis of the data, based on **Equation (1)**, yielded a Stern-Volmer constant, K_{sv} = 246.68 M^{-1}. The fluorescence lifetime of **3a**, τ_0, was previously determined as being 7.83 ns. Using this lifetime, the quenching constant was found to be $k_q = 3.15 \times 10^{10}\ M^{-1}\ s^{-1}$. The good correlation coefficient obtained leads us to believe that, apparently, a linear behaviour was followed.

$$\frac{I_0}{I} = \left(1 + K_{SV}[Q]\right) = \left(1 + k_q\tau_0[Q]\right) \qquad \textbf{(1)}$$

However, a more detailed study of the Stern-Volmer plot shows that this linearity was not in fact apparent at a low concentration of F^-. As can be seen in Figure 8, the linear behaviour of the Stern-Volmer equation was not observed on the titration of **3a**. This observation can be stated, not only to this experiment, but to all our other experiments. The deviation of the Stern-Volmer equation from linearity can be explained if we consider an alternative quenching process to the dynamic quenching. Hence, the quenching of the fluorescence emission can also arise from static quenching, which can be considered to be due to the interaction between the receptor and the sensor in the ground state, prior to excitation, or dynamic quenching, with formation of a complex between the excited sensor, and the anion receptor. Because of this, both the static and dynamic quenching effects were taken into account in the modified Stern-Volmer equation, **Equation (2)**, where k_s is an equilibrium constant for the static quenching. [31]

$$\frac{I_0}{I} = \left(1 + K_{SV}[Q]\right)\left(1 + k_S[Q]\right) = 1 + \left(k_S + k_q\tau_0\right)[Q] + k_S k_q \tau_0 [Q]^2 \qquad (2)$$

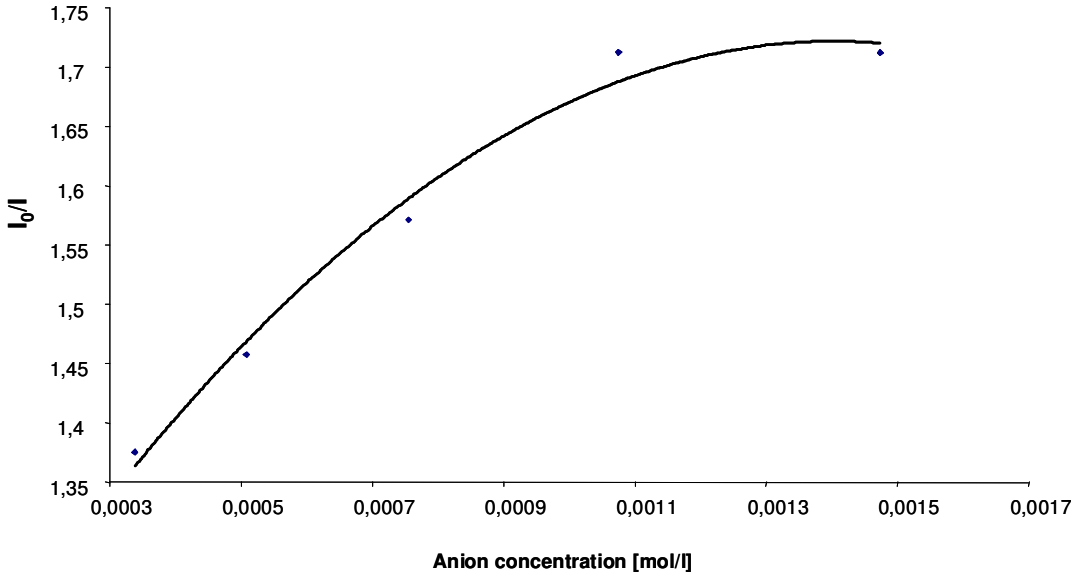

Figure 8. Fraction of the Stern-Volmer plot for the fluorescence quenching of **3a** upon anion, F^-, titration

Using this equation, the kinetics of the fluorescence quenching were re-fitted, by using τ_0, 7.83×10^{-9} s and both the dynamic and static quenching constants, k_q and k_s, determined. For these changes, the values for k_q and k_s were found to be: $k_q = 3.09 \times 10^{10}$ M^{-1} s^{-1}, $k_s = 0.22$ M^{-1}. Even though these are not very significant, from what we observed above, the results do suggests the presence of the static quenching which implies that the sensor is interacting with the anion both in the ground and excited state with a dynamic quenching rate constant close to the diffusion controlled values.

In order to differentiate the dynamic quenching constant obtained using **Equation (1)** from the one obtained using **Equation (2)**, the terms k_{qsv} and k_q were used respectively. The values of K_{sv} and consequently k_{qsv} (dynamic quenching constant based on $K_{sv} = k_{qsv}\ \tau_0$), k_q and k_s found for the fluorescence titrations of **3a-d** with F^-, I^-, AcO^- and $H_2PO_4^-$, following the same method, are summarised in **Table 1**. Since the lifetimes are not dependent on the static quenching, the fluorescence lifetimes shown in **Table 1** for **3a-3d** as a function of the anion concentrations have been measured and analysed according to the **Equation (3)**, where τ_0 and τ are respectively the lifetimes in the absence and presence of quencher (same as reported above).

$$\frac{\tau_0}{\tau} = 1 + k_q \tau_0 [Q] \qquad (3)$$

Table 1. Results form the kinetic investigation for the anion induced quenching of **3a-3d.**

Sensor	τ_0 [ns]	Anion	K_{sv} [M^{-1}]	k_{qsv} [$M^{-1}s^{-1}$]	k_q [$M^{-1}s^{-1}$]	k_s [M^{-1}]
3a	7.83	F^-	246.68	3.15×10^{10}	3.09×10^{10}	0.22
		I^-	79.17	1.01×10^{10}	4.63×10^{9}	9.77
		AcO^-	25.11	3.21×10^{9}	3.67×10^{9}	1.42.*
		$H_2PO_4^-$	8.86	1.79×10^{9}	4.47×10^{9}	6.91 *

3b	8.99	F^-	773.66	8.61×10^{10}	1.27×10^{11}	8.43 *
		I^-	58.68	6.53×10^{9}	4.08×10^{9}	6.03
		AcO^-	93.72	1.04×10^{10}	1.63×10^{10}	7.55 *
		$H_2PO_4^-$	35.02	3.9×10^{9}	7.73×10^{9}	8.84 *
3c	1.32	F^-	158.31	1.2×10^{11}	2.68×10^{11}	9.14 *
		I^-	14.78	1.12×10^{10}	1.34×10^{10}	1.11 *
		AcO^-	59.41	4.5×10^{10}	8.89×10^{10}	13.53 *
		$H_2PO_4^-$	24.67	1.87×10^{10}	2.6×10^{10}	3.82 *
3d	4.96	F^-	452.87	9.13×10^{10}	1.19×10^{11}	3.87 *
		I^-	25.99	5.24×10^{9}	6.91×10^{9}	2.21 *
		AcO^-	99.09	1.2×10^{10}	2.04×10^{10}	0.45 *
		$H_2PO_4^-$	24.94	5.03×10^{9}	9.8×10^{9}	7.89 *

K_{sv} and consequently k_{qsv}, k_q and k_s values found for the fluorescence titrations of **3a-d** with F^-, I^-, AcO^- and $H_2PO_4^-$. *All these values were taken as module as the values were found, following the method described above, to be negative.

From the results in Table 1, it is clear that the fluoride anion gives rise to large $\mathbf{K_{SV}}$, even though its value changes dramatically within this set of sensors. Moreover, these values are about an order of magnitude greater than diffusion control. This is, probably due to, and as discussed earlier, the fact that the there is some degree of ion pairing of bifluoride with the recptor. With the exception of I^-, which has significant ground state interactions with the fluorophores, the same order was observed (as expected) as above with $AcO^- > H_2PO_4^-$. These results also show that the quenching is on all occasion fast and dominated by dynamic quenching, except at low concentrations.

CONCLUSION

We have synthesised several new simple fluorescent PET anion sensors, **3a-d**. These were characterised using conventional techniques as well as the crystal structure of the dimerized [4π+4π] photocycloaddition product of **3b**. These sensors display 'ideal' PET behaviour upon

anion recognition, since only the fluorescence emission is "*switched off*" in the presence of $H_2PO_4^-$, AcO^-, and F^- in DMSO. Hence, the changes in the ground state were only minor and occurred at short wavelengths, which we associate with the interactions of the anions with the receptor, which modulates the receptors redox potential. These sensors also showed good selectivity with AcO^- being recognised over $H_2PO_4^-$. Nevertheless, **3a-d** all showed higher affinity and more efficient quenching for F^-. This is not all together surprising since fluoride high charge density and small size enables it to form strong hydrogen bonds with the urea receptor. Moreover, the anion can deprotonate the receptors, forming HF_2^- which makes the receptor a significantly stronger electron donor and hence an efficient quencher. We also observed significant changes for the titration of I^-. However, these were deemed to be mainly due to ground state interactions between the sensor and the anion. The absorption spectra of all the sensors were shifted to longer wavelengths in comparison to anthracene. Moreover, all the sensors, with the exception of **3c**, gave rise to larger quantum yields of fluorescence, and were also red shifted. A more detailed evaluation of the quenching process using the Stern-Volmer equation showed that generally the expected linearity was up held confirming dynamic quenching. However, closer examination for all the anions showed that at lower anion concentration, static quenching was also observed.

ACKNOWLEDGMENTS

We thank Trinity College Dublin, Universidade de Coimbra, and IRCSET for financial support. We also like to thank Dr. John E. O'Brien for his help.

EXPERIMENTAL

General:

Reagents (obtained from Aldrich) and solvents were purified using standard techniques. Melting points were determined using a GallenKamp melting point apparatus. Infrared spectra were recorded on a Mattson Genesis II FTIR spectrophotometer equipped with a Gateway 2000 4DX2-66 workstation. ^{1}H NMR spectra were recorded at 400 MHz using a Bruker Spectrospin DPX-400 instrument. ^{13}C NMR spectra were recorded at 100 MHz using a Bruker Spectrospin DPX-400 instrument.

Spectroscopic studies:

All measurements were made at room temperature. Fluorescence spectra were measured using a Jovin Ivon-Spex-Fluorolog 3-2.2; the excitation wavelength was 369 nm, the excitation and emission slit widths were 0.5 mm. Emission spectra were corrected for the instrumental response of the system. The absorption spectra were recorded on a Shimadzu UV-2100 spectrophotometer. All absorption and fluorescence spectra were obtained from a solution of the sensor in DMSO in both the absence and the presence of anion guests. The effect of anions on the sensors was investigated by addition of different volumes of an anion (Br^-, Cl^-, I^-, F^-, AcO^-, $H_2PO_4^-$) solution in DMSO, with different concentrations (10^{-5}M to 1M), to a 2ml solution of **3a-d** in DMSO. In each case, for the fluorescence spectra, additions were accompanied with magnetic stirring. All titrations were repeated two times to ensure reproducibility. All the anions were used in the form of their tetrabutylammonium salts [(TBA), $(C_4H_9)_4N^+$]. These salts were purchased from Aldrich and used without further purification. DMSO was purchased from Riedel-Häen and stored over molecular sieves prior to use.

Fluorescence decay measurements were carried out using a home-built TCSPC apparatus with an N_2 filled IBH 5000 coaxial flash lamp as excitation source, Jobin-Ivon monochromators, Philips XP2020Q photomultiplier, and Canberra instruments TAC and MCA. [32, 33] Alternate measurements (1000 c.p.c.) of the pulse profile at 356 nm and the sample emission were performed until 1-2 × 10^4 counts at the maximum were reached. The fluorescence decays were analyzed using the modulating functions method of Striker with automatic correction for the photomultiplier "wavelength shift" [34]. The method used to determine the fluorescence quantum yields of compounds **3a-d** (Φ_F^C) involve a connection between the fluorescence quantum yield of a reference (Φ_F^{ref}) and Φ_F^C. Anthracene was the reference used (Φ_F^{ref} = 0.27, in ethanol (EtOH), [35]). Firstly absorbance of the reference, in EtOH, and compounds, in DMSO, were adjusted to similar values (below 0.10) at the excitation wavelength. After this, the fluorescence spectra were recorded, under identical experimental conditions, and a comparison was made between the integrated areas under the fluorescence spectra of both the reference and the compounds. At last the **Equation (4)** was followed in order to obtain the Φ_F^C values [35], where A_{ref} and A_C are respectively the

$$\Phi_F^C = [(A_{ref}\, F_C\, n^2_C)/(\, A_C\, F_{ref}\, n^2_{ref})]\, \Phi_F^{ref} \quad \textbf{(4)}$$

absorbance of reference and compounds at the excitation wavelength, F_C is the integrated emission area of the compounds ($\int I(\lambda)^C\, d\lambda$) and F_{ref} is the integrated emission area of the reference spectra ($\int I(\lambda)^{ref}\, d\lambda$), n_C and n_{ref} are respectively the refraction index of the solvent containing the compound (DMSO), n_{DMSO} =1.4793 and the reference (EtOH), n_{DMSO} =1.3611. [27]

Synthesis:

9-Aminomethyl anthracene, **1** (0.1 g, $4.83x10^{-4}$mol) was dissolved in ca. 5 mL of freshly distilled dry CH_2Cl_2. To this solution 1.1 equivalent of the appropriate isocyanate in a single portion was added. Off-white or light yellow precipitates were immediately formed upon addition of the isocyanate. The reaction was allowed to stir for several hours, before the precipitate was isolated by filtration, washed with dry CH_2Cl_2 and dried under high vacuum (over P_2O_5) and eventually recrystallised from $CHCl_3$ to give powders.

1-Anthracen-9-ylmethyl-3-(2,4-difluoro-phenyl)-urea (3a)

Was obtained as an off-white solid in 80% yield. MS (ES^+) m/z = 385.11 [M + Na]. Calculated for $C_{22}H_{16}N_2OF_2Na$ [M+Na] m/z = 385.1128. Found m/z = 385.1111. Anal.Calcd for $C_{22}H_{16}N_2OF_2$: C, 72.92; H, 4.45; N, 7.73; Found: C, 72.67; H, 4.45; N, 7.62%. ^{1}H-NMR (400 MHz, DMSO-d_6): δ_H, 8.63 (s, 1H, AnthrCH), 8.47 (s, 1H, NH), 8.45 (s, 1H, NH), 8.18 (m, 4H, ArCH), 8.12 (s, 2H, AnthrCH), 7.64 (t, 2H, AnthrCH, *J* = 8 Hz), 7.56 (t, 2H, AnthrCH, *J* = 8.04 Hz), 7.21 (m, 1H, ArCH), 7.10 (m, 1H, AnthrCH), 7.02 (t, 1H, ArCH, *J* = 9.04 Hz), 5.33 (d, 2H, CH_2, *J* = 5 Hz); ^{13}C- NMR (100 MHz, $CDCl_3$): δ_C, 154.61, 152.59, 150.05, 131.09, 130.38, 129.69, 128.99, 127.37, 126.49, 125.30, 124.86, 124.82, 124.72, 124.28, 120.98, 120.89, 110.99, 110.78, 103.79, 103.52, 103.29, 35.15.

1-Anthracen-9-ylmethyl-3-tolyl-urea (3b)

Was obtained as an off-white solid in 84% yield, mp 215-218^{o}C; Calculated for $C_{17}H_{16}N_2S$:C, 72.82%; H, 5.75%; N, 9.99%; Found C, 70.01%; H, 4.30%; N, 7.05%; ^{1}H-NMR (400 MHz, $CDCl_3$): δ_H, 8.68 (s, 1H, Ar-10H), 8.64 (s, 2H, Ar-4H, Ar-5H), 8.49 (d, 2H, *J* = 9.0 Hz, Ar-1H, Ar-8H), 8.15 (d, 2H, *J* = 8.5 Hz, Ar-3H, Ar-6H), 7.65 (q, 2H, J_1 = 6.5 Hz, J_2 = 7.5 Hz, Ar-18H, Ar-22H), 7.56 (d, 2H, *J* = 7.0 Hz, Ar-3H, Ar-6H), 5.35 (s, 2H, 15-H, *J* = 3 Hz); ^{13}C- NMR (100 MHz, $CDCl_3$): δ_C, 160, 138.57, 131.85, 131.29, 130.55,

129.76, 128.88, 128.76, 126.99, 125.32, 125.08, 124.01, 123.92, 120.50, 57.43; ^{19}F NMR: 66.96; IR (KBr) cm^{-1} 3427, 3342, 2922, 1641, 1550, 1330, 729.

1-Anthracen-9-ylmethyl-3-(3,5-dimethyl-phenyl)-urea (3c)

Was obtained as an off-white solid in 80% yield. MS (ES$^+$) m/z = 377.16 [M + Na]. Calculated for $C_{24}H_{22}N_2ONa$ [M+Na] m/z = 377.1630. Found m/z = 377.1637. Calculated for $C_{24}H_{22}N_2O$: C, 81.33; H, 6.26; N, 7.90; Found: C, 80.63; H, 6.11; N, 7.81%. ^{1}H-NMR (400 MHz, DMSO-d_6): δ_H, 8.62 (s, 1H, AnthrCH), 8.47 (d, 2H, AnthrCH, *J* = 9.04 Hz), 8. 14 (s, 1H, NH), 8.12 (s, 2H, AnthrCH), 7.63 (t, 2H, AnthrCH, *J* = 9.04 Hz), 7.55 (t, 2H, AnthrCH, *J* = 8.04 Hz), 6.99 (s, 2H, ArCH), 6.61 (s, 1H, NH), 6.54 (s, 1H, ArCH), 5.30 (d, 2H, CH_2, *J* = 5 Hz), 2.19 (s, 6H, CH_3); ^{13}C-NMR (100 MHz, $CDCl_3$): δ_C, 171.74, 170.39, 170.20, 162.40, 145.05, 142.18, 123.88, 119.03, 57.29, 54.63, 54.52, 53.04, 36.30, 35.77, 35.65, 35.23, 35.14, 35.08.

1-Anthracen-9-ylmethyl-3-phenyl-urea (3d)

Was obtained as an off-white solid 77% yield. mp 209-210^{o}C; Calculated for $C_{22}H_{17}N_2O$:C, 80.96%; H, 5.56%; N, 8.58%; found C, 80.96%; H, 5.55%; N, 8.59%; ^{1}H-NMR (400 MHz, DMSO-d_6): δ_H, 8.15 (s, 1H, Ar-10H), 7.96(d, 2H, *J* = 9.0 Hz, Ar-1H, Ar-8H), 7.89 (s, 2H, , Ar-4H, Ar-5H), 7.64 (s, 2H, Ar-18H, Ar-22H), 7.38 (d, 2H, *J* = 9.0 Hz, Ar-2H, Ar-7H), 7.37(d, 2H, *J* = 8.0 Hz, Ar-3H, Ar-6H), 7.24 (s, 2H, Ar-19H, Ar-21H), 7.09 (s, 1H, Ar-20H), 4.86 (s, 2H, Ar-15H); ^{13}C-NMR (100 MHz, $CDCl_3$): δ_C, 160, 138.53, 131.91, 131.26, 130.56, 129.76, 128.94, 128.67, 126.81, 125.35, 125.06, 124.01, 123.92, 120.50, 54.41.

References:

[1] J. F. Callan, A.P. de Silva, D.C. Magri, *Tetrahedron,* **2005**, *36*, 8551; See special issue on Fluorescent Sensors: *J. Mater. Chem*., **2005**, *15*, 2617-2976.

[2] deSilva, A.P.; Gunaratne, H.Q.N.; Gunnlaugsson, T.; Huxley, A. J. M.; McCoy, C. P.; Rademacher J. T.; Rice, T. E. *Chem. Rev*. **1997**, *97*, 1515.

[3] Gunnlaugsson, T.; Leonard J.P. *Chem. Commun*. **2005**, 3114. (b) Leonard J.P.; Gunnlaugsson T. *J. of. Fluoresc.* **2005**, *15*, 585.

[4] Sessler, J. L.; Gale, P. A.; Cho, W. S., *Anion Receptor Chemistry*; Royal Society of Chemistry: Cambridge, UK.

[5] Steed, J. W., *Chem. Commun*., **2006**, 2637; Martínez-Máñez, R. Sancenón, F. *Chem. Rev*, **2003**, *103*, 4419. Suksai, C.; Tuntulani, T. *Chem. Soc. Rev*., **2003**, *32***,** 192.

[6] Gale, P.A. *Coord. Chem. Rev.,* **2001**, *213*, 79; Gale, P.A. *Coord. Chem. Rev.,* **2000**, *199*, 181; Beer P.D.; Gale, P.A. *Angew. Chem. Int. Ed.,* **2001**, *40*, 486.

[7] Gale, P. A., *Acc. Chem. Res*., **2006**, *39*, 465. Gale P. A. *Chem. Commun*., **2005**, 3761.

[8] Matthews, S. E.; Beer, P. D., *Supramol. Chem*., **2005**, *17*, 411; Davis A. P., Joos J. B., *Coord. Chem. Rev*., **2003**, ***240*,** 143.

[9] Gunnlaugsson, T.; Glynn, M.; Tocci (née Hussey), G. M.; Kruger, P. E.; Pfeffer, F. M. *Coord. Chem. Rev*., **2006**, *250*, 3094; Gunnlaugsson, T.; Ali H.D.P.; Glynn, M.; Kruger, P.E.; Hussey G. M. Pfeffer F. M.; dos Santos, C. M. G.; Tierney, J.; *J. of. Fluoresc.*, **2005**, *15,* 287.

[10] Bianchi, E. Bowman-James, K. García-España, E. Eds. *Supramolecular Chemistry of Anions*, Wiley-VCH, New York, 1997.

[11] Light, M.E.; Gale, P.A.; Navakhun, K.; Quesada, R. *Chem. Commun.*, **2006**, 901; Brooks, S. J.; Edwards, P. R.; Gale, P. A.; Light, M. E. *New. J. Chem*. **2006**, *30*, 65; Brooks, S. J.; Gale, P. A.; Light, M. E. *Chem. Commun.* **2005**, 4696.

[12] Brooks, S. J.; Gale, P. A.; Light, M. E. *Chem. Commun.* **2006**, 4344.

[13] Pfeffer, F. M,; Seter, M.; Lewcenko, N.; Barnett, N. W. *Tetrahedron Lett.,* **2006**, *47*, 5241; Pfeffer F. M.; Buschgens, A. M.; Barnett, N. W.; Gunnlaugsson, T.; Kruger, P. E., *Tetrahedron Lett.,* **2005**, *46*, 6579; Pfeffer, F. M.; Gunnlaugsson, T.; Jensen, P.; Kruger, P.E., *Org. Lett*. **2005**, *7*, 5375.

[14] Wel L. H.; He, Y. B.; Wu, J. L.; Wu, X. J.; Meng, L., Yang, X. *Supramol. Chem.,* **2004**, *16*, 561.

[15] Gómez D. E., Fabbrizzi, L., Licchelli, M., Monzani, E. *Org. Biomol. Chem*., **2005**, *3*, 1495; Boiocchi, M.; Boca, L.D.; Gómez, D.E.; Fabbrizzi, L.; Licchelli, M.; Monzani, E. *J. Am. Chem. Soc.*, **2004**, *126*, 16507.

[16] Wu, F.Y.; Li, Z.; Gua, L.; Wang, X.; Lin, M.H.; Zhao, Y.F.; Jiang, J.B. *Org. Biomol. Chem*. **2006**, *4*, 624; Wen, Z.C.; Jiang, Y.B. *Tetrahedron,* **2004**, *60*,11109; Wu, F.Y.; Li, Z.; Wen, Z.C.; Zhou, N.; Zhao, Y.F.; Jiang, Y.B. *Org. Lett*., **2002**, *4*, 3202.

[17] Gunnlaugsson, T.; Davis, A.P.; Glynn, M. *Chem. Commun*., **2001**, 2556; Gunnlaugsson, T. Davis, A.P. Hussey, G. M. Tierney, J. Glynn, M. *Org. Biomol. Chem*., **2004**, *2*, 1856; Gunnlaugsson, T.; Davis, A. P.; O'Brien, J. E.; Glynn M., *Organic Lett.* **2002**, *4*, 2449; Gunnlaugsson, T.; Davis, A. P.; O'Brien, J. E.; Glynn, M. *Org. Biomol. Chem.*, **2005**, *3,* 48.

[18] Quinlan E.; Matthews S. E.; Gunnlaugsson, T., *Tetrahedron Lett.,* **2006**, *47*, 9333.

[19] Gunnlaugsson, T.; Kruger, P. E.; Lee, T. C.; Parkesh, R.; Pfeffer, F. M.; Hussey**,** G. M.; *Tetrahedron Lett.*, **2003**, *44*, 6575.

[20] Harte, A. J.; Jensen, P.; Plush, S. E.; Kruger, P. E.; Gunnlaugsson, T.; *Inorg. Chem.* **2006**, *45*, 9465; Gunnlaugsson, T.; Harte, A. J.; Leonard, J. P.; Nieuwenhuyzen, M. *Supramol. Chem.* **2003**, *15*, 505; Gunnlaugsson, T.; Harte, A. J.; Leonard, J. P.; Nieuwenhuyzen, M. *Chem. Commun.* **2002**, 2134.

[21] Leonard, J. P.; dos Santos, C. M. G.; Plush, S. E.; McCabe, T., Gunnlaugsson, T. *Chem. Commun*., **2006**, **DOI:** 10.1039/b611487c

[22] Parkesh, R.; Lee, T. C.; Gunnlaugsson, T. *Org. Biomol. Chem*., **2007**, *5*, 310; Gunnlaugsson, T.; Leonard J. P.; Murrey, N.S. *Organic. Lett*, **2004**, 6, 1557; Gunnlaugsson, T.; Harte, A. J.; Leonard J. P.; Senegal, K. *Chem. Commun.*, **2004**, 782; Gunnlaugsson, T.; Lee C. T.; Parkesh, R. *Organic. Lett*, **2003**, *5*, 4065; Gunnlaugsson, T.; Lee, T. C.; Parkesh, R. *Org. Biomol. Chem*., **2003**, *1*, 3265; Gunnlaugsson, T.; Bichell, B.; Nolan, C. *Tetrahedron Lett*., **2002**, *43*, 4989; Gunnlaugsson, T.; Nieuwenhuyzen, M.; Ludovic R.; Vera T. *Tetrahedron Lett.,*, **2001,** *42***,** 4725; de Silva, A. P.; Gunaratne, H. Q. N.; Gunnlaugsson, T.; Nieuwenhuyzen, M. *Chem. Commun.*, **1996**, 1967.

[23] The data were collected on a Bruker Smart Apex Diffractometer*. The crystal was mounted on 0.35mm quartz fibre and immediately placed on the goniometer head in a 123K N2 gas stream. The data was acquired using Smart Version 5.625 software in multi-run mode and 2400 frames in total, at 0.3^{o} per frame, were collected. Data integration and reduction was carried out using Bruker Saint+ Version 6.45 software and corrected for absorption and polarization effects using Sadabs Version 2.10 software. Space group determination, structure solution and refinement were obtained using Bruker Shelxtl Ver. 6.14 software. SMART Software Reference Manual, version 5.625, Bruker Analytical X-Ray Systems Inc., Madison, WI, 2001. Sheldrick, G. M. SHELXTL, An Integrated System for Data Collection, Processing, Structure Solution and Refinement, Bruker Analytical X-Ray Systems Inc., Madison, WI, 2001.

[24] ***Crystal data*:-** C25 H23 F3 N2 O2 S, Monoclinic, space group C2/c, a = 31.430(3), b = 8.7283(9), c = 16.3151(17) Å, β = 97.952(2)^{o}, U = 4432.6(8) Å^{3}, T = 123 K, μ (Mo–Kα) = 0.191mm^{-1}, Z = 8, A total of 14403 reflections were measured for 4 < 2Θ <57 and 3169 unique reflections were used in the refinement, [R(int) = 0.0391], the final parameters were wR2 = 0.1102 and R1 = 0.0466[I>2σ(I)]. CCDC 627537.

[25] Bouas-Laurent, H.; Castellan, A., Desvergne, J.-P.; Lapouyade, R. *Chem. Soc, Rev.,* **2001**, *30*, 248; Bouas-Laurent, H.; Castellan, A., Desvergne, J.-P.; Lapouyade, R. *Chem. Soc, Rev.,* **2000**, *29*, 43.

[26] Molard, Y.; Bassani, D. M.; Desvergne, J.-P.; Moran, N.; Tucker, J. H. R. *J. Org. Chem.,* **2006**, *71*, 8523.

[27] Murov, S. L.; Carmichael, I.; Hug, G. L. *Handbook of Photochemistry*, 2nd ed.; Marcel Dekker, Inc.: New York, 1993.

[28] Martell, A. E.; Motekaitis, R. J. *The determination and use of stability constants*; VCH Publishers: Weinheim, 1988.

[29] Gunnlaugsson, T.; Kruger, P.E.; Jensen, P.; Pfeffer, F. M.; Hussey, G. M. *Tetrahedron Lett.*, **2003**, *44* 8909.

[30] Kang, S.O.; Powell, D.; Day, V.W.; Bowman-James, K. *Angew. Chem. Int. Ed.*, **2006**, *45*, 1921.

[31] Lordeiro, C.; Pina, F.; Parola, A. J.; Bencini, A.; Bianchi, A.; Bazzicalupi, C.; Ciattini, S.; Giorgi, C.; Masotti, A.; Valtancoli, B.; Seixas de Melo, J. *Inorg. Chem.*, **2001**, *40*, 6813; Amire, S. A; Burrows, H. D.; *J. Chem. Soc., Faraday Trans. 1*, **1982**, *78*, 2033; Rehm, D.; Weller, A. *Israel J. Chem.*, **1970,** *8*, 259 – 271.

[32] Seixas de Melo, J.; Silva, L. M.; Kuroda, M. *J. Chem. Phys.*, **2001,** *115*, 5625.

[33] Seixas de Melo, J.; Fernandes, P. F. *J. Mol. Struct.*, **2001,** *565 – 566*, 69.

[34] Stricker, G.; Subramaniam, V.; Seidel, C. A. M.; Volkmer, A. *J. Phys. Chem. B*, **1999**, *103*. 8612.

[35] Ramachandram, B.; Samanta, A. *Chem. Phys. Let.*, **1998,** *290*, 9.

Figures for Prof. Gunnlaugsson Supramol. Chem. 2007

Figure 1:

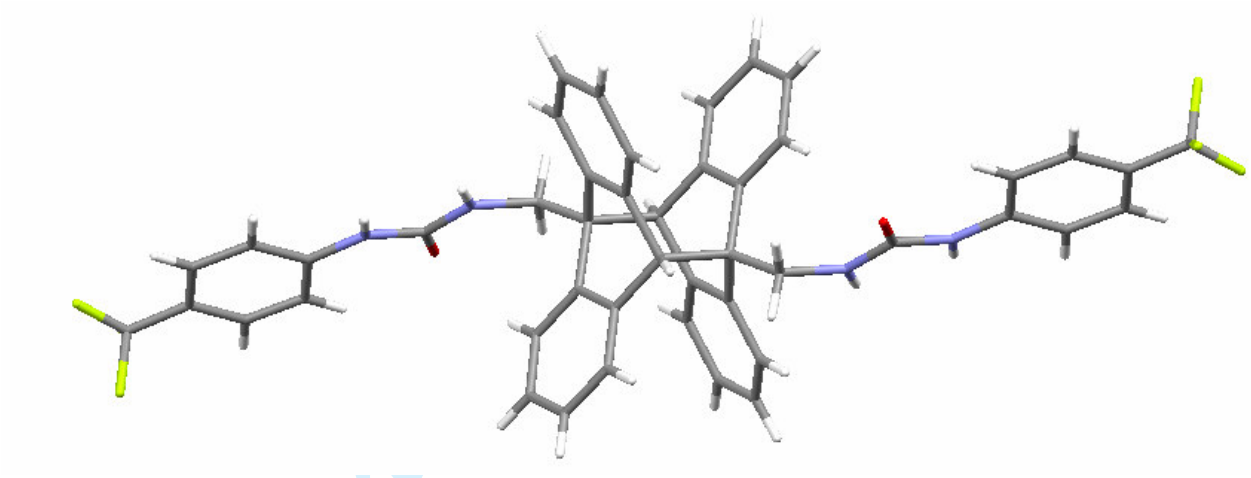

Figure 2:

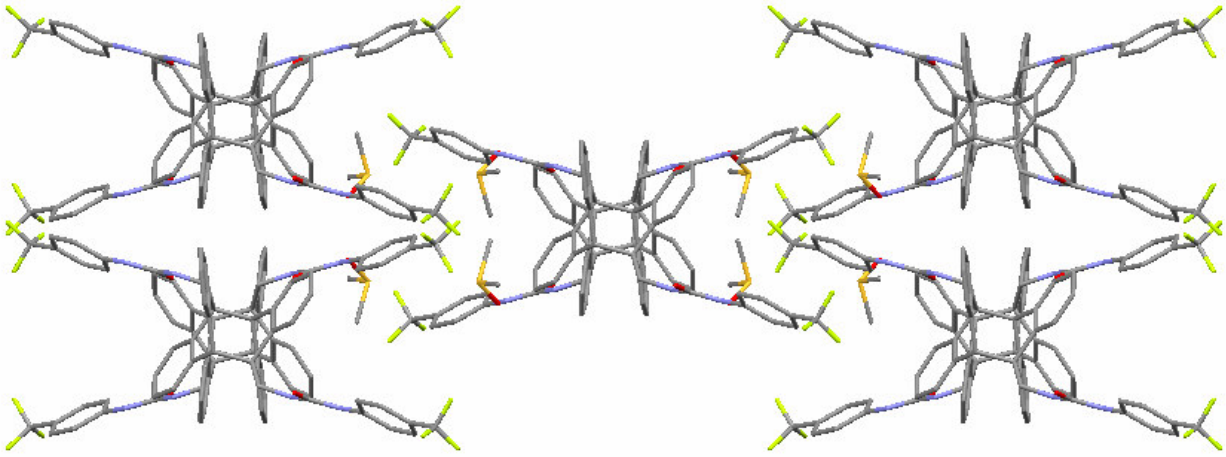

Figure 3

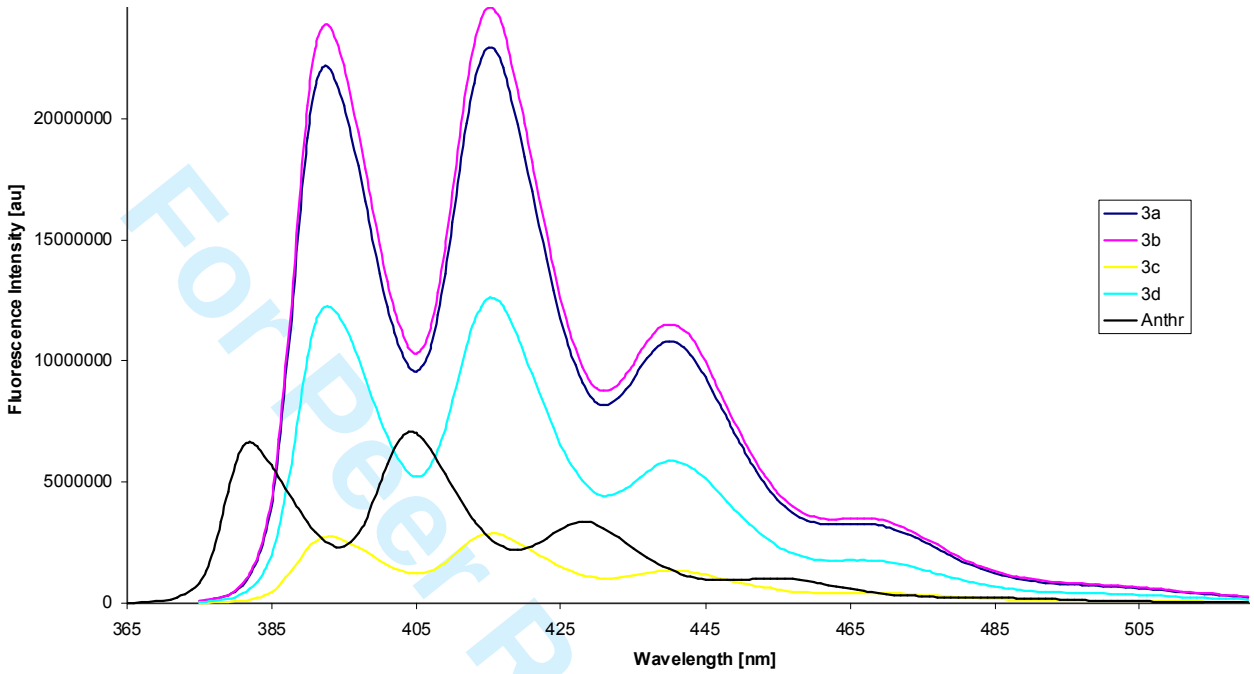

Figure 4

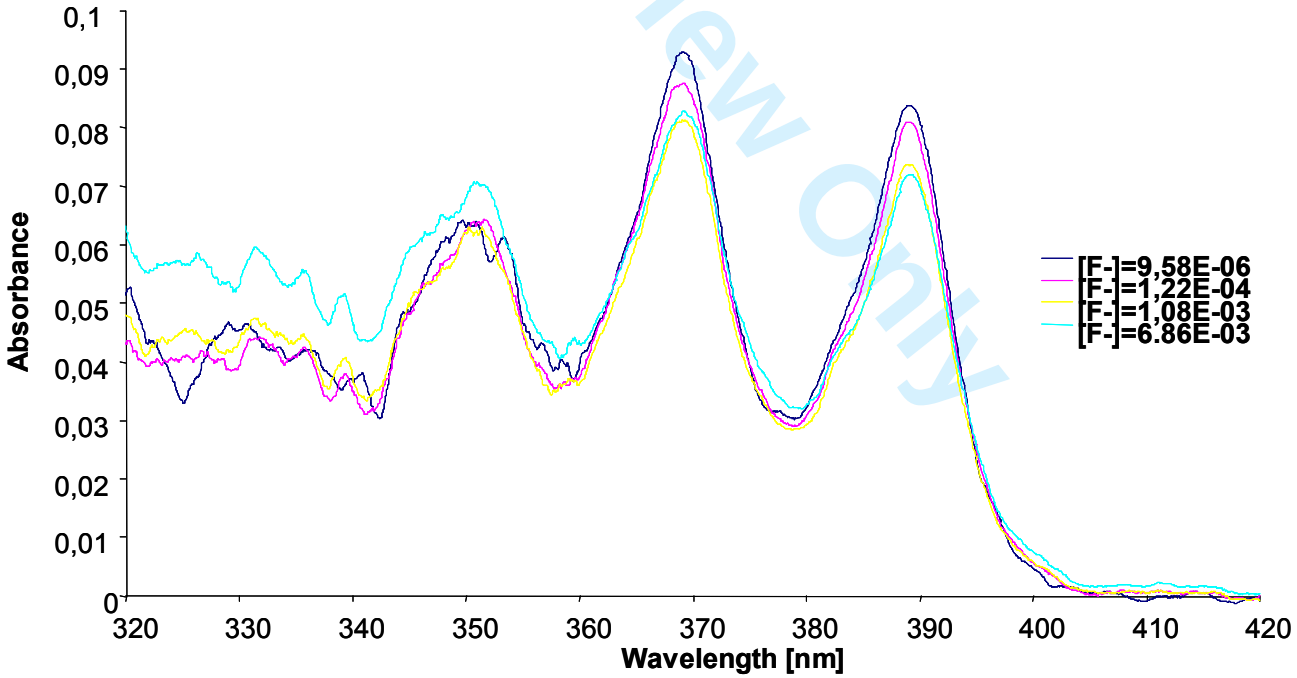

Figure 5:

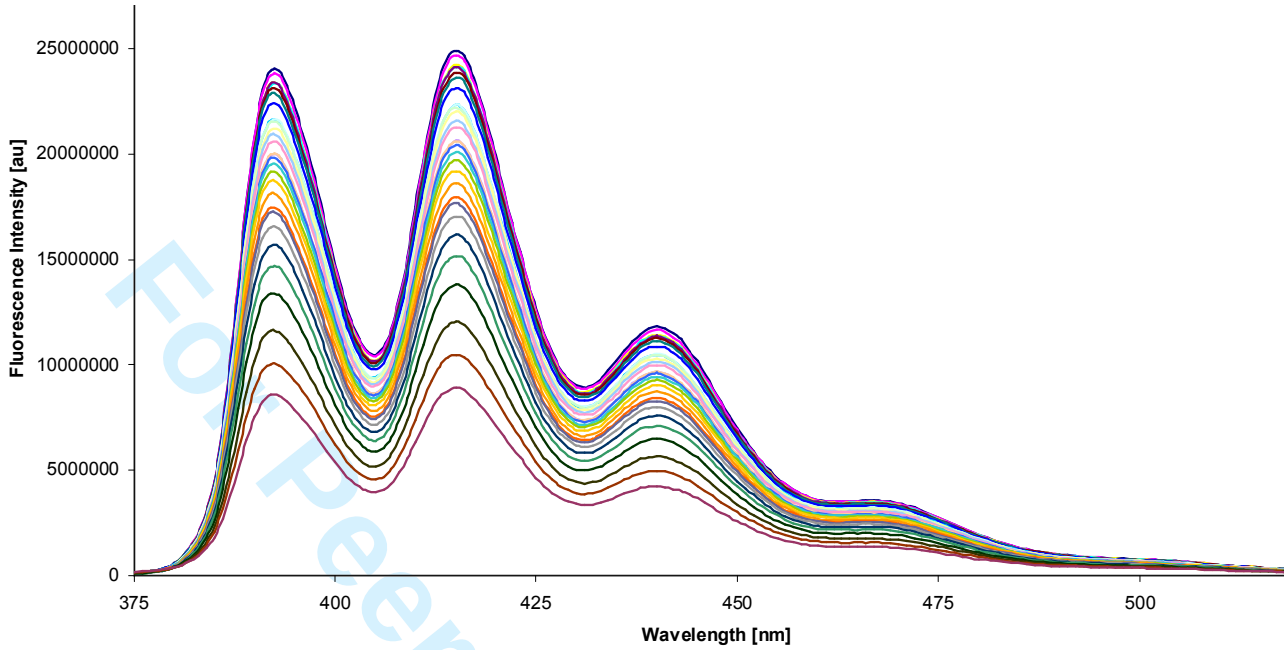

Figure 6:

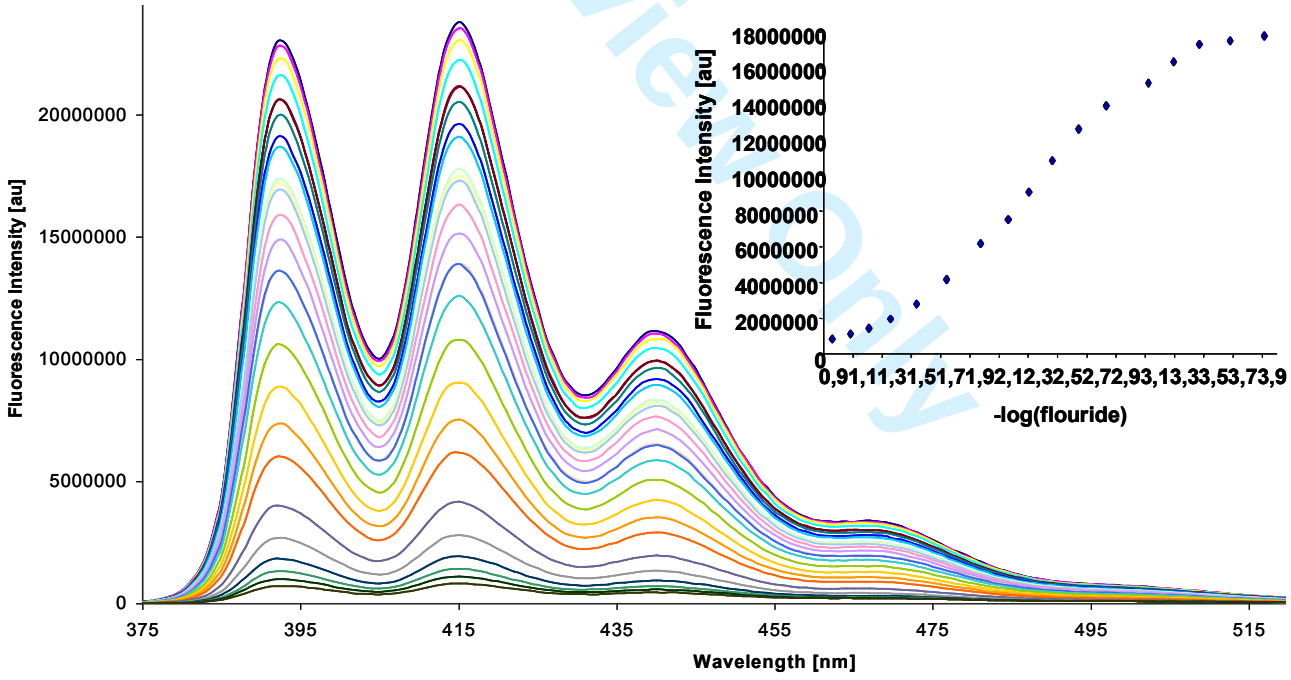

Figure 7:

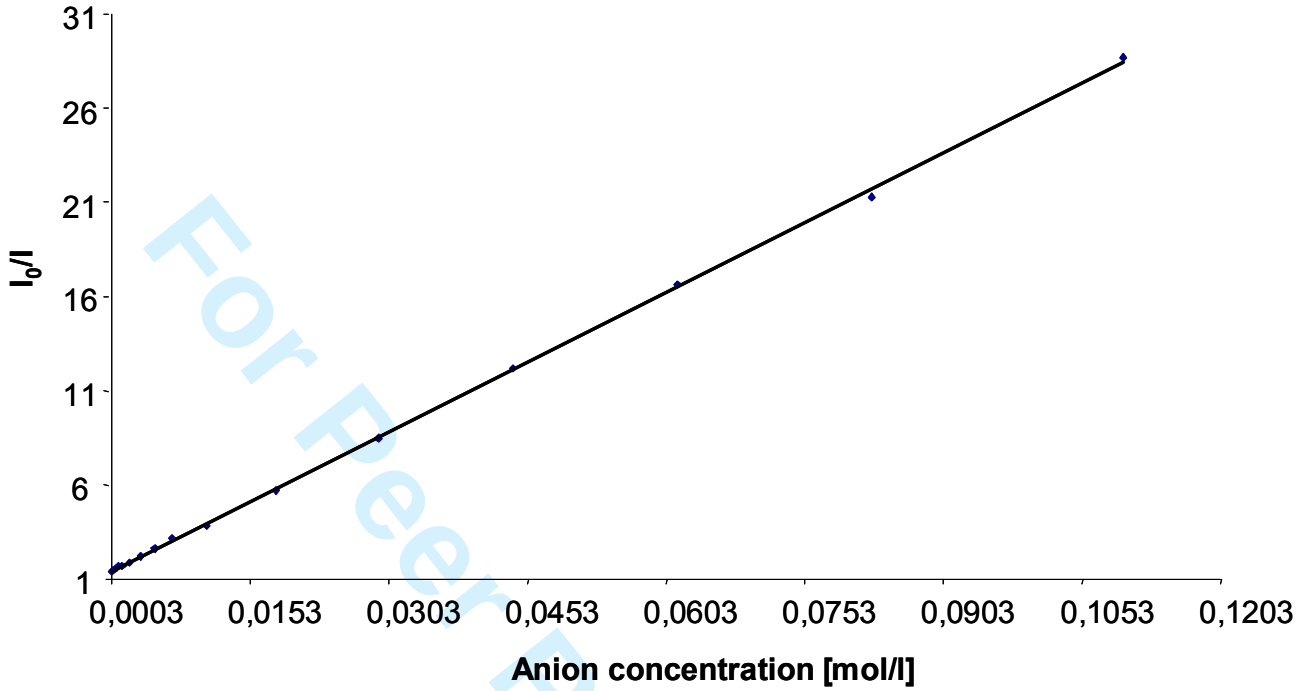

Figure 8: